---

**Article:**
Bate, Fiona, Billingham, J, King, A C et al. (1 more author) (2006) An asymptotic theory for the propagation of a surface-catalysed flame in a tube. Journal of Fluid Mechanics. pp. 363-393. ISSN 1469-7645

https://doi.org/10.1017/S0022112005007172

---

# An asymptotic theory for the propagation of a surface-catalysed flame in a tube

By F. ADAMSON[1], J. BILLINGHAM[2], A. C. KING[1] AND K. KENDALL[3]

[1]Department of Mathematics and Statistics, The University of Birmingham, Edgbaston, Birmingham B15 2TT, UK

[2]School of Mathematical Sciences, The University of Nottingham, University Park, Nottingham NG7 2RD, UK

[3]Department of Chemical Engineering, The University of Birmingham, Edgbaston, Birmingham B15 2TT, UK

(Received 4 March 2005)

Experiments have shown that when a mixture of fuel and oxygen is passed through a zirconia tube whose inner surface is coated with a catalyst, and then ignited at the end of the tube, a reaction front, or flame, propagates back along the tube towards the fuel inlet. The reaction front is visible as a red hot region moving at a speed of a few millimetres per second. In this paper we study a model of the flow, which takes into account diffusion, advection and chemical reaction at the inner surface of the tube. By assuming that the flame propagates at a constant speed without change of form, we can formulate a steady problem in a frame of reference moving with the reaction front. This is solved using the method of matched asymptotic expansions, assuming that the Reynolds and Damköhler numbers are large. We present numerical and, where possible, analytical results, firstly when the change in fluid density is small (a simplistic but informative limit) and secondly in the fully compressible case. The speed of the travelling wave decreases as the critical temperature of the surface reaction increases and as the mass flow rate of fuel increases. We also make a comparison between our results and some preliminary experiments.

## 1. Introduction

In this paper we construct and analyse a mathematical model for a novel, surface-catalysed reaction front that has been observed in an experiment performed recently on a model fuel cell (Lefevre 2003). The experimental set up is shown in Figure 1. A mixture of fuel and oxygen is fed into one end of a long thin tube of zirconia (the inlet). The opposite end of the tube (the outlet) is heated by igniting the gas so as to form a premixed flame at the end of the tube. The increased temperature at the outlet starts a reaction on the inner surface of the zirconia, where a high surface area platinum catalyst is present, and the heat produced by the reaction causes the tube to glow red. When the premixed flame at the end of the tube is extinguished, the red glow remains, and then moves at a speed of a few millimetres per second along the tube towards the inlet. The motion of the reaction front is shown in Figure 2; fuel flows along the tube from the left and the outlet is at a distance shown by $d = 90$ mm on the ruler. The speed of the reaction front calculated from these pictures is about 0.46 mm $s^{-1}$. This speed decreases as the flow rate of fuel coming into the tube increases, and increases with the amount of catalyst on the inner surface of the tube. There is an obvious analogy between

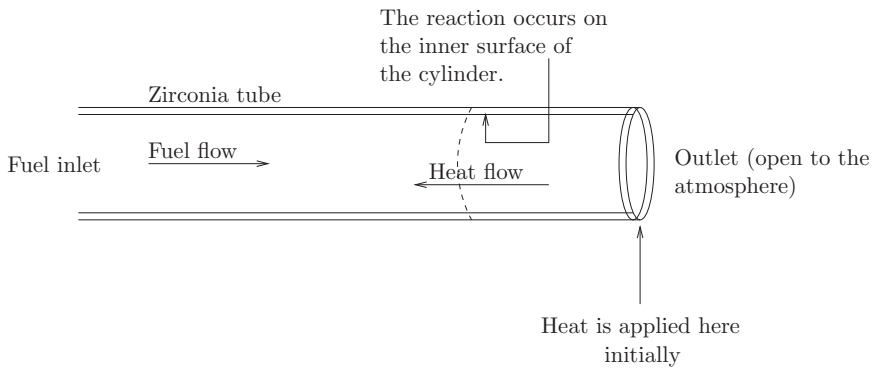


FIGURE 1. Schematic of the experiment.

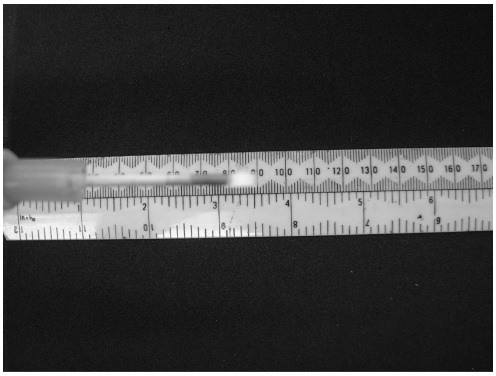

(a) At time $t = 0.0$ s the reaction front is at $d = 80$ mm.

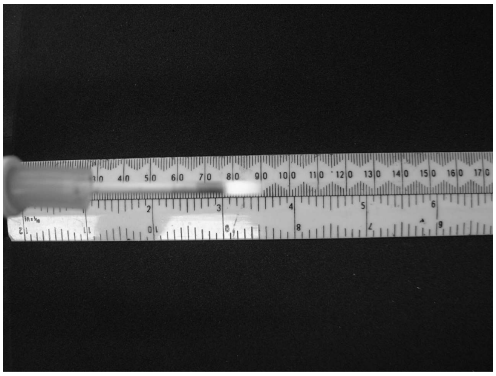

(b) At time $t = 6.5$ s the reaction front has progressed to $d = 77$ mm.

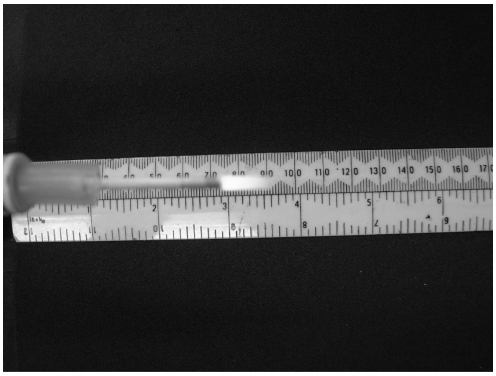

(c) At time $t = 12.7$ s the reaction front has progressed to $d = 74$ mm.

FIGURE 2. The observed propagation of the reaction front, or surface-catalysed flame.

this phenomenon and the classical experiment of Davy (1817). In his experiment, Davy heated a fine platinum wire and introduced it into a mixture of methane and air. He noted:

"...the oxygene (sic) and coal gas in contact with the hot wire combined without

flame, and yet produced heat enough to preserve the wire ignited, and to keep up their own combustion."

Apart from its intrinsic scientific interest, an understanding of surface-catalysed flames could improve our understanding of the way a fuel cell behaves as it is heated to its working temperature. A fuel cell is a device that converts chemical energy into electrical energy. It differs from a battery in that it is continuously supplied with fuel rather than simply using a finite amount of fuel stored within it. The fuel cell is one of the cleanest and most efficient forms of energy production available at the moment (Winkler 1994; Kumar, Krumpelt and Myles 1992). There are several types of fuel cell in development which have different applications. The solid oxide fuel cell (SOFC) consists of an electrolyte layer made from a solid ceramic, zirconia ($ZrO_2$), which at high temperatures (usually at least $700^oC$) can conduct oxygen ions (Singhal and Kendall 2003). Fuel reacts on one side of the zirconia, where a catalyst is present, reducing the oxygen concentration on this side. The other side, which is exposed to the air, remains at the atmospheric oxygen concentration. The fuel burning process therefore results in a gradient in oxygen concentration across the zirconia electrolyte. An electrical connection is placed across the zirconia, the cathode on the oxygen rich side and the anode on the fuel side. At the cathode, electrons combine with oxygen molecules to form negatively charged oxygen ions, which travel through the zirconia down the concentration gradient. On reaching the anode, the oxygen ions release electrons and react with fuel. The electrons continue around the circuit back to the cathode.

An important design feature of the SOFC is that the oxygen rich and fuel sides of the electrolyte must be kept separate. This ensures that the oxygen travels only through the electrolyte and produces an electrical current. Any leakage of oxygen between the two sides of the fuel cell reduces its efficiency. The tubular SOFC is made up of a tube of zirconia with tubular electrodes on either side. This arrangement helps to solve the problem of sealing one side from the other. The tubular design we study was developed by Kendall and Prica (1994) and Finnerty *et al* (1998). Fuel flows through the zirconia tube and reacts with oxygen at the inner surface which is coated with a platinum catalyst. The tubes used in these cells are extruded from powders dispersed in polymer solutions which makes the cells more resistant to thermal and mechanical shocks. These cells can therefore be used for small scale applications as they are not likely to break during rapid start-up.

Previous mathematical analysis of the tubular SOFC has considered the cell running under isothermal steady state conditions (Cooper 2000; Cooper, Billingham and King 2000). The surface-catalysed reaction front that we study here is relevant to the initial heating and start-up of this type of fuel cell. We shall neglect electrochemical effects in our analysis, since the surface catalysed reaction front is observed in the absence of electrochemical activity. In the following section we formulate a mathematical model that describes the flow field, temperature distribution and mass fraction distributions, and the speed of the reaction front. We then describe the basic structure of the asymptotic solution, and some of the boundary value problems that we need to solve, in Section 3. We take two different approaches: in Section 4 we consider the case of small heat production, and hence constant density at leading order, whilst in Section 5 we present results for the fully compressible model, which has a slightly more involved asymptotic structure. We then compare our theory with some preliminary experiments, and draw some conclusions.

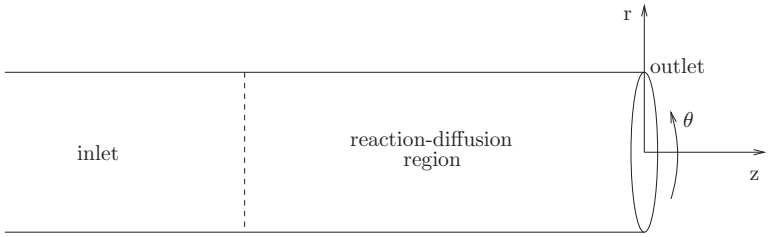


FIGURE 3. The coordinate system and asymptotic regions.

## 2. The mathematical model

In the following analysis we use a cylindrical polar coordinate system, $(r, \theta, z)$, with the origin at the centre of the outlet of the tube, as shown in Figure 3. Although we formulate the governing equations for an unsteady flow, in due course we shall look for a steady, permanent form travelling wave solution (a flame solution).

### 2.1. *The governing equations*

The equations for conservation of mass, momentum and energy can be derived using continuum theory for a mixture of reacting species (Buckmaster and Ludford 1982). We will work with the mass averaged velocity of the fluid, $\mathbf{u}$, and the mass fractions, $Y_i$, of the separate reacting species. These are defined so that the density of species $i$ is $\rho Y_i$ where $\rho$ is the total density of the fluid mixture. The mass conservation equation for species $i$ is

$$\rho\left(\frac{\partial Y_i}{\partial t} + \mathbf{u}\cdot\boldsymbol{\nabla} Y_i\right) = \boldsymbol{\nabla}\cdot\left(\rho D \boldsymbol{\nabla} Y_i\right), \tag{2.1}$$

where $D$ is the molecular diffusivity of the gases in the mixture, which we assume to be the same for each species. The equation for conservation of total mass is

$$\frac{\partial \rho}{\partial t} + \boldsymbol{\nabla}\cdot(\rho\mathbf{u}) = 0. \tag{2.2}$$

Note that the right hand side is zero, since the temperature of the mixture is low enough that there is no significant chemical reaction in the bulk. The chemical reaction is confined to the inner surface of the tube, where a platinum catalyst is present, and will therefore appear as a boundary condition.

Since the chemical reaction does not occur in the bulk, there is no creation of momentum or energy there and the mixture of gases just behaves as a continuous fluid. Conservation of momentum is

$$\frac{\partial \mathbf{u}}{\partial t} + \mathbf{u}\cdot\boldsymbol{\nabla}\,\mathbf{u} = \frac{1}{\rho}\,\boldsymbol{\nabla}\cdot\boldsymbol{\sigma}, \tag{2.3}$$

where $\boldsymbol{\sigma}$ is the stress tensor,

$$\boldsymbol{\sigma} = -p\mathbf{I} + \mu\left(\boldsymbol{\nabla}\mathbf{u} + (\boldsymbol{\nabla}\mathbf{u})^T\right) - \frac{2}{3}\,\mu\,(\boldsymbol{\nabla}\cdot\mathbf{u})\,\mathbf{I},$$

and $\mathbf{I}$ is the unit tensor. The parameter $\mu$ is the mass averaged kinematic viscosity of the fluid mixture and $p$ is the pressure. Conservation of energy is

$$\rho c_p \frac{\mathrm{D}T}{\mathrm{D}t} = \frac{\mathrm{D}p}{\mathrm{D}t} - \frac{2}{3}\mu\,(\boldsymbol{\nabla}\cdot\mathbf{u})^2 + \mu\left(\boldsymbol{\nabla}\mathbf{u} + (\boldsymbol{\nabla}\mathbf{u})^T\right) : \boldsymbol{\nabla}\mathbf{u} + \boldsymbol{\nabla}\cdot(k\boldsymbol{\nabla}T), \tag{2.4}$$

where $T$ is the temperature of the fluid mixture, $c_p$ is the heat capacity at constant pressure and $k$ is the thermal conductivity of the mixture.

| Physical quantity | Symbol | Value/magnitude | |
|---|---|---|---|
| inner radius of tube | $a$ | $10^{-3}$ | m |
| width of tube | $h = b - a$ | $2 \times 10^{-4}$ | m |
| mass flow rate at inlet | $q_{\text{in}}$ | $1 \times 10^{-6}$ | kg s$^{-1}$ |
| inlet (room) temperature | $T_{\text{in}}$ | 293 | K |
| critical temperature of reaction | $T_c$ | $O(10^3)$ | K |
| density at the inlet ($T = T_{\text{in}}$) | $\rho_{\text{in}}$ | $O(1)$ | kg m$^{-3}$ |
| molecular diffusivity at inlet | $D_{\text{in}}$ | $O(10^{-6})$ | m$^2$ s$^{-1}$ |
| viscosity of gas mixture at inlet | $\mu_{\text{in}}$ | $O(10^{-5})$ | kg m$^{-1}$ s$^{-1}$ |
| thermal conductivity of gas mixture at inlet | $k_{\text{in}}$ | $O(10^{-2})$ | W m$^{-1}$ K$^{-1}$ |
| specific heat at constant pressure of gas mixture | $c_p$ | $O(10^3)$ | J kg$^{-1}$ K$^{-1}$ |
| specific heat at constant volume of gas mixture | $c_v$ | $O(10^3)$ | J kg$^{-1}$ K$^{-1}$ |
| Stefan-Bolzman constant | $\sigma$ | $5.67 \times 10^{-8}$ | W m$^{-2}$ K$^{-4}$ |
| emissivity of zirconia tube | $\epsilon$ | $O(10^{-1})$ | |
| surface heat transfer coefficient | $H$ | $O(1)$ | W m$^{-2}$ K$^{-5/4}$ |
| heat of combustion of methane | $Q_c$ | $5.570 \times 10^7$ | J kg$^{-1}$ |
| rate of reaction | $k_0$ | $O(10^{-2})$ | m s$^{-1}$ |

TABLE 1. Parameters, their values and their meanings.

We assume that the separate gases all satisfy the equation of state for a perfect gas so that

$$p_i = \frac{R\rho Y_i T}{m_i},$$

where $R$ is the molar gas constant and $m_i$ is the molecular mass of species $i$. From this, Dalton's law of partial pressures gives the total pressure, $p$, in terms of the mass fractions, $Y_i$, as

$$p = R\rho T \sum_{i=1}^{N} \frac{Y_i}{m_i}.$$

### 2.2. *Boundary conditions and initial simplifications*

In order to obtain an asymptotic solution that will provide us with some insight into the structure of the flow, we must make some simplifying assumptions. We first look to simplify the chemistry of the problem. The reaction of methane with oxygen is complex (Senkan 1992) and we simplify the system so that the reaction is essentially

$$\text{fuel} \rightarrow \text{products}.$$

This model is widely used for premixed flames (Buckmaster and Ludford 1982). Since mass is conserved, $m_f = m_p$, where the subscripts $f$ and $p$ denote properties of the fuel and product respectively. Also, since the sum of the mass fractions is always unity, we have $Y_p = 1 - Y_f$ and hence we only have to solve for the fuel mass fraction which satisfies

$$\rho\left(\frac{\partial Y_f}{\partial t} + u\frac{\partial Y_f}{\partial r} + w\frac{\partial Y_f}{\partial z}\right) = \frac{1}{r}\frac{\partial}{\partial r}\left(r\rho D\frac{\partial Y_f}{\partial r}\right) + \frac{\partial}{\partial z}\left(\rho D\frac{\partial Y_f}{\partial z}\right). \tag{2.5}$$

This simplification also affects the equation of state, which becomes

$$p = \frac{R\rho T}{m_f}.$$

Chemical reaction takes place on the inner surface of the tube only, since this is the only place where the catalyst is present. At the boundary between the surface of the tube and the rest of the gas, $r = a$, there is an influx of fuel into the boundary, balanced by an efflux of products produced by the chemical reaction. Using the law of mass action, we have

$$\rho D \frac{\partial Y_f}{\partial r} = \begin{cases} -k_0 \rho Y_f, & T > T_c, \\ 0, & T < T_c, \end{cases} \qquad \text{at} \quad r = a,$$

where $k_0$ is the rate of the catalysed reaction, which we take to be constant. We have also assumed that no reaction takes place when the temperature at the surface of the tube is below the critical temperature, $T_c$. Surface catalysis is a complicated process and this is a reasonable first approximation of what happens.

At the inner surface of the tube there are several other boundary conditions. Continuity of velocity normal to the surface gives $u = 0$ at $r = a$, since gases cannot penetrate the tube wall. The no slip condition at the solid boundary is $w = 0$ at $r = a$. To obtain the heat flux boundary condition, we assume that the radial temperature gradient across the tube is small, since the zirconia is thin compared to the radius of the tube. We can therefore combine the boundary conditions at $r = a$, the inner surface, and $r = b$, the outer surface, to obtain

$$k \frac{\partial T}{\partial r} + \sigma \epsilon \left( T^4 - T_{\text{in}}^4 \right) + H \left( T - T_{\text{in}} \right)^{5/4} = \begin{cases} k_0 \rho Y_f Q_c, & T > T_c, \\ 0, & T < T_c, \end{cases} \qquad \text{at} \quad r = a,$$

where $\sigma$ is the Stefan Bolzman constant, $\epsilon$ and $H$ are the emissivity and coefficient of surface heat transfer of zirconia respectively and $Q_c$ is the heat of combustion of methane. The second and third terms on the left hand side of the equation give the heat loss by radiation and natural convection respectively (Carslaw and Jaeger 1959). The magnitudes of these heat losses can be estimated using the non-dimensional radiation heat transfer coefficient, $A = O(10^{-2})$, and the Nusselt number, $Nu = O(10^{-1})$ (see Tables 1 and 2). Since these heat losses are small in comparison to the magnitude of the heat flux through the tube, we will neglect them here, although their effect on the solution as a small perturbation over a long distance remains to be investigated. In particular, the appearence of the reaction front as a red band rather than an extended red hot region must be due to cooling by heat losses. We assume that this affects the appearence, but not the leading order behaviour of the flame.

The length of the tube is much greater than its radius, so we treat it as semi-infinite to leading order. The temperature, mass fraction and mass flow rate at the inlet therefore satisfy

$$T \to T_{\text{in}}, \quad Y_f \to 1, \quad 2\pi \int_0^a \rho w r \, \mathrm{d}r \to q_{\text{in}} \quad \text{as} \quad z \to -\infty, \tag{2.6}$$

where $q_{\text{in}}$ is the inlet mass flow rate and $T_{\text{in}}$ the inlet temperature.

### 2.3. *Non-dimensionalisation*

In what follows, dimensional variables are denoted by a star. We non-dimensionalise the governing equations using characteristic scales of the system. As there is now no geometrical length scale in the axial direction, we use the diffusion length scale. The

dimensionless variables are

$$r = \frac{r^*}{a}\,, \qquad z = \frac{z^*}{qa}\,, \qquad u = \frac{qu^*}{W}\,, \qquad w = \frac{w^*}{W}\,, \qquad t = \frac{Wt^*}{qa}\,, \qquad T = \frac{T^*}{T_{\rm in}}\,,$$
$$k = \frac{k^*}{k_{\rm in}}\,, \qquad D = \frac{D^*}{D_{\rm in}}\,, \qquad \mu = \frac{\mu^*}{\mu_{\rm in}}\,, \qquad p = \frac{p^* - p_{\rm in}}{\rho_{\rm in} W^2}\,, \qquad \rho = \frac{\rho^*}{\rho_{\rm in}}\,,$$

where $qa$ is the diffusion length scale and

$$q = \frac{Wa}{D_{\rm in}}.$$

The parameters $D_{\rm in}$, $\mu_{\rm in}$, $k_{\rm in}$ and $\rho_{\rm in}$ are the diffusivity, viscosity, thermal conductivity and density of the mixture of fluids at the inlet temperature, $T_{\rm in}$. The axial velocity scale, $W$, is given by

$$W = \frac{q_{\rm in}}{\pi a^2 \rho_{\rm in}}.$$

In terms of these variables, the dimensionless governing equations are

$$\frac{\partial \rho}{\partial t} + \frac{1}{r}\frac{\partial}{\partial r}(r\rho u) + \frac{\partial}{\partial z}(\rho w) = 0, \tag{2.7a}$$

$$\frac{\partial u}{\partial t} + u\frac{\partial u}{\partial r} + w\frac{\partial u}{\partial z} = -q^2\frac{1}{\rho}\frac{\partial p}{\partial r} + \frac{q}{Re}\frac{1}{3\rho}\left[4\frac{\partial}{\partial r}\left(\mu\frac{\partial u}{\partial r}\right) + 4\frac{\mu}{r}\frac{\partial u}{\partial r} - \frac{4u\mu}{r^2} + 3\frac{\partial}{\partial z}\left(\mu\frac{\partial w}{\partial r}\right) - 2\frac{\partial}{\partial r}\left(\mu\frac{\partial w}{\partial z}\right) - 2\frac{u}{r}\frac{\partial \mu}{\partial r}\right] + \frac{1}{Re\,q}\frac{1}{\rho}\frac{\partial}{\partial z}\left(\mu\frac{\partial u}{\partial z}\right), \tag{2.7b}$$

$$\frac{\partial w}{\partial t} + u\frac{\partial w}{\partial r} + w\frac{\partial w}{\partial z} = -\frac{1}{\rho}\frac{\partial p}{\partial z} + \frac{1}{Re\,q}\frac{1}{3\rho}\left[\frac{1}{r}\mu\frac{\partial u}{\partial z} + 3\frac{\partial}{\partial r}\left(\mu\frac{\partial u}{\partial z}\right) - 2\frac{\partial}{\partial z}\left(\mu\frac{\partial u}{\partial r}\right) + 4\frac{\partial}{\partial z}\left(\mu\frac{\partial w}{\partial z}\right) - 2u\frac{1}{r}\frac{\partial \mu}{\partial z}\right] + \frac{q}{Re}\frac{1}{\rho}\frac{1}{r}\frac{\partial}{\partial r}\left(r\mu\frac{\partial w}{\partial r}\right), \tag{2.7c}$$

$$\rho\left(\frac{\partial Y_f}{\partial t} + u\frac{\partial Y_f}{\partial r} + w\frac{\partial Y_f}{\partial z}\right) = \frac{1}{r}\frac{\partial}{\partial r}\left(r\rho D\frac{\partial Y_f}{\partial r}\right) + \frac{1}{q^2}\frac{\partial}{\partial z}\left(\rho D\frac{\partial Y_f}{\partial z}\right), \tag{2.7d}$$

$$\begin{aligned}\rho\left(\frac{\partial T}{\partial t} + u\frac{\partial T}{\partial r} + w\frac{\partial T}{\partial z}\right) &= M^2(\gamma-1)\left(\frac{\partial p}{\partial t} + u\frac{\partial p}{\partial r} + w\frac{\partial p}{\partial z}\right)\\ &+\frac{M^2(\gamma-1)}{q\,Re}\mu\left(-\frac{2}{3}\left[\frac{1}{r}\frac{\partial}{\partial r}(ru) + \frac{\partial w}{\partial z}\right]^2\right.\\ &\left.+2\left[\left(\frac{\partial u}{\partial r}\right)^2 + \left(\frac{u}{r}\right)^2 + \left(\frac{\partial w}{\partial z}\right)^2 + 2\frac{\partial u}{\partial z}\frac{\partial w}{\partial r}\right]\right)\\ &+\frac{M^2(\gamma-1)}{q^3\,Re}\mu\left(\frac{\partial u}{\partial z}\right)^2 + \frac{M^2(\gamma-1)q}{Re}\mu\left(\frac{\partial w}{\partial r}\right)^2\\ &+\mathcal{L}\frac{1}{r}\frac{\partial}{\partial r}\left(rk\frac{\partial T}{\partial r}\right) + \frac{\mathcal{L}}{q^2}\frac{\partial}{\partial z}\left(k\frac{\partial T}{\partial z}\right),\end{aligned} \tag{2.7e}$$

$$p = \frac{1}{\gamma M^2}\left(\rho T - 1\right), \tag{2.7f}$$

| Symbol | Definition | Typical value | Description |
|---|---|---|---|
| $q$ | $\dfrac{q_{\rm in}}{\pi a \rho_{\rm in} D_{\rm in}}$ | $O(10^2)$ | $\dfrac{\text{rate of fuel flow}}{\text{rate of diffusion}}$ |
| $Re$ | $\dfrac{q_{\rm in}}{\pi a \mu_{\rm in}}$ | $O(10^2)$ | $\dfrac{\text{inertial forces}}{\text{viscous forces}}$ |
| $Pr$ | $\dfrac{\mu_{\rm in} c_p}{k_{\rm in}}$ | $O(1)$ | $\dfrac{\text{momentum diffusivity}}{\text{thermal diffusivity}}$ |
| $\mathcal{L}$ | $\dfrac{k_{\rm in}}{\rho_{\rm in} D_{\rm in} c_p}$ | $O(1)$ | $\dfrac{\text{thermal diffusivity}}{\text{mass diffusivity}}$ |
| $\gamma$ | $\dfrac{c_p}{c_v}$ | $O(1)$ | $\dfrac{\text{specific heat at constant pressure}}{\text{specific heat at constant volume}}$ |
| $M$ | $\dfrac{q_{\rm in}}{\pi a^2 \rho_{\rm in}\sqrt{(\gamma-1)\, c_p T_{\rm in}}}$ | $O(10^{-3})$ | $\dfrac{\text{average speed in fluid}}{\text{average speed of sound in fluid}}$ |
| $Q$ | $\dfrac{Q_c}{c_p T_{\rm in}}$ | $O(10)$ | $\dfrac{\text{heat produced in reaction}}{\text{heat transferred by conduction}}$ |
| $Da$ | $\dfrac{k_0\, a}{D_{\rm in}}$ | $O(10)$ | $\dfrac{\text{rate of reaction}}{\text{rate of diffusion}}$ |
| $\varepsilon$ | $\dfrac{h}{a}$ | $O(10^{-1})$ | $\dfrac{\text{thickness of tube}}{\text{radius of tube}}$ |
| $A$ | $\dfrac{\sigma \epsilon T_{\rm in}^3 a}{k_{\rm in}}$ | $O(10^{-2})$ | $\dfrac{\text{rate of heat transfer by radiation}}{\text{rate of heat transfer by conduction}}$ |
| $Nu$ | $\dfrac{Ha T_{\rm in}^{1/4}}{k_{\rm in}}$ | $O(10^{-1})$ | $\dfrac{\text{rate of heat transfer by convection}}{\text{rate of heat transfer by conduction}}$ |

TABLE 2. The dimensionless parameters.

where $Re$ and $\mathcal{L}$ are the Reynolds number and Lewis number respectively, defined by

$$Re = \frac{W a \rho_{\rm in}}{\mu_{\rm in}}, \qquad \mathcal{L} = \frac{k_{\rm in}}{\rho_{\rm in} D_{\rm in} c_p}.$$

The parameter $M$ is the Mach number given by $M = W/w_s$ where $w_s = \sqrt{(\gamma-1)\, c_p T_{\rm in}}$ is the speed of sound through the fluid and $\gamma$ is the ratio of specific heats, $\gamma = c_p/c_v$. Since $M^2 \ll 1$ (see Table 2), we will set $M = 0$ in all future calculations. Defining the Prandtl number by $Pr = \mu_{\rm in} c_p / k_{\rm in}$ we can write $q$ in terms of the Reynolds, Prandtl and Lewis numbers as

$$q = Re\, Pr\, \mathcal{L}. \tag{2.8}$$

Since both $Pr$ and $\mathcal{L}$ are $O(1)$ parameters, $q = O(Re)$, with $Re \gg 1$. We can therefore think of $q$ as a measure of the mass flow rate.

2.3.1. *Boundary conditions*

In terms of the dimensionless variables, the boundary conditions at $r = 1$ are

$$u = 0, \qquad\qquad w = 0,$$

$$\rho D\frac{\partial Y_f}{\partial r} = \begin{cases} -Da\rho Y_f, & T > T_c, \\ 0, & T < T_c, \end{cases} \qquad\qquad k\frac{\partial T}{\partial r} = \begin{cases} QDa\rho Y_f/\mathcal{L}, & T > T_c, \\ 0, & T < T_c, \end{cases}$$

where $T_c$ is now the dimensionless critical temperature of the reaction, $Da$ is the Damköhler number and $Q$ is the dimensionless heat of reaction

$$Da = \frac{k_0 a}{D_{\text{in}}}, \qquad\qquad Q = \frac{Q_c}{c_p T_{\text{in}}}.$$

At $r = 0$, $u$, $w$, $Y_f$ and $T$ must be finite, and

$$u \to 0, \quad w \sim \text{inlet velocity}, \quad Y_f \to 1, \quad T \to 1, \quad \int_0^1 r\rho w \,\mathrm{d}r \to \frac{1}{2},$$

as $z \to -\infty$.

2.4. *Further simplifications*

A commonly used, and reasonable approximation is that the fuel and temperature diffuse at the same rate, and hence that the Lewis number is unity, $\mathcal{L} = 1$ (Buckmaster and Ludford 1982). From this we further assume that the temperature dependences of the thermal conductivity and diffusion coefficient are such that

$$k = \rho D.$$

This allows us to add $Q$ times (2.7d) to (2.7e) and obtain

$$\rho\left(\frac{\partial}{\partial t}(QY_f + T) + u\frac{\partial}{\partial r}(QY_f + T) + w\frac{\partial}{\partial z}(QY_f + T)\right) = \frac{1}{r}\frac{\partial}{\partial r}\left(rk\frac{\partial}{\partial r}(QY_f + T)\right) + \frac{1}{q^2}\frac{\partial}{\partial z}\left(k\frac{\partial}{\partial z}(QY_f + T)\right).$$

From the boundary conditions we have

$$\frac{\partial}{\partial r}(QY_f + T) = 0, \qquad\qquad \text{at} \quad r = 1,$$

and

$$QY_f + T \to Q + 1, \qquad\qquad \text{as} \quad z \to -\infty,$$

so $QY_f + T = Q + 1$ is a solution. We therefore only have to explicitly solve for one of either temperature or mass fraction. We choose to solve for temperature.

## 3. The structure of the asymptotic solution

We now seek an asymptotic structure based on the limit of large $q$ and $Da$. Physically, this corresponds to a rapid throughput of fuel and fast chemical reaction at the inner surface of the tube. We look for a travelling wave solution, which we expect will develop as the large time solution. We transform the equations into a frame of reference moving with the flame front at a constant speed, $c$, which we will have to determine. Experimentally

this wave speed is much less than the flow speed and its magnitude will be determined theoretically by the scalings in the asymptotic regions, as we will show in Section 3.1. Writing $z' = z + ct$ and substituting into (2.7), we obtain

$$\frac{1}{r}\frac{\partial}{\partial r}(r\rho u) + \frac{\partial}{\partial z'}(\rho w') = 0, \tag{3.1a}$$

$$u\frac{\partial u}{\partial r} + w'\frac{\partial u}{\partial z'} = -q^2\frac{1}{\rho}\frac{\partial p}{\partial r} + \frac{q}{Re}\frac{1}{3\rho}\left[4\frac{\partial}{\partial r}\left(\mu\frac{\partial u}{\partial r}\right) + 4\frac{\mu}{r}\frac{\partial u}{\partial r} - \frac{4u\mu}{r^2} + 3\frac{\partial}{\partial z'}\left(\mu\frac{\partial w'}{\partial r}\right) - 2\frac{\partial}{\partial r}\left(\mu\frac{\partial w'}{\partial z'}\right) - 2\frac{u}{r}\frac{\partial \mu}{\partial r}\right] + \frac{1}{Re\,q}\frac{1}{\rho}\frac{\partial}{\partial z'}\left(\mu\frac{\partial u}{\partial z'}\right), \tag{3.1b}$$

$$u\frac{\partial w'}{\partial r} + w'\frac{\partial w'}{\partial z'} = -\frac{1}{\rho}\frac{\partial p}{\partial z'} + \frac{1}{Re\,q}\frac{1}{3\rho}\left[\frac{1}{r}\mu\frac{\partial u}{\partial z'} + 3\frac{\partial}{\partial r}\left(\mu\frac{\partial u}{\partial z'}\right) - 2\frac{\partial}{\partial z'}\left(\mu\frac{\partial u}{\partial r}\right) + 4\frac{\partial}{\partial z'}\left(\mu\frac{\partial w'}{\partial z'}\right) - 2u\frac{1}{r}\frac{\partial \mu}{\partial z'}\right] + \frac{q}{Re}\frac{1}{\rho}\frac{1}{r}\frac{\partial}{\partial r}\left(r\mu\frac{\partial w'}{\partial r}\right), \tag{3.1c}$$

$$\rho\left(u\frac{\partial T}{\partial r} + w'\frac{\partial T}{\partial z'}\right) = \frac{1}{r}\frac{\partial}{\partial r}\left(rk\frac{\partial T}{\partial r}\right) + \frac{1}{q^2}\frac{\partial}{\partial z'}\left(k\frac{\partial T}{\partial z'}\right), \tag{3.1d}$$

$$\rho T = 1, \tag{3.1e}$$

where $w' = w + c$ is the axial velocity in the new frame of reference. The boundary conditions in this frame of reference become

$$u = 0, \qquad w' = c,$$

$$k\frac{\partial T}{\partial r} = \begin{cases} Da\rho\,(Q + 1 - T), & z' > 0, \\ 0, & z' < 0, \end{cases} \qquad \text{at} \quad r = 1. \tag{3.2}$$

At $r = 0$ we require that $u$, $w'$ and $T$ are finite, and as $z' \to -\infty$ we match the flow in the reaction region to the steady inlet flow. In order to fix the axes in the flame, we assume that the surface catalysed reaction is not active for $z' < 0$, so that the temperature at $z' = 0$ is the critical temperature, $T_c$. Since the Damköhler number is large, changes in the flow due to the reaction occur in a small region close to the reaction front at $z' = 0$, $r = 1$. This region is the innermost of our asymptotic structure and is shown as region IV in Figure 4. The outer regions, I and II, give the $O(1)$ flow in the tube for $z' < 0$ and $z' > 0$ respectively. In $z' < 0$, no chemical reaction occurs and the flow at leading order is just the steady inlet flow. In $z' > 0$, changes in the flow due to chemical reaction at $r = 1$ diffuse out into the centre of the tube. The solution in region III matches together the solutions in regions II and IV.

In regions I and II, the leading order equations are the large $q$ and $Da$ limits of (3.1) and (3.2). From (2.8) we have $q = PrRe$, since $\mathcal{L} = 1$. Substituting this into (3.1) and taking the limit of large $q$ we have,

$$\frac{1}{r}\frac{\partial}{\partial r}(r\rho u) + \frac{\partial}{\partial z'}(\rho w') = 0, \tag{3.3a}$$

$$\frac{\partial p}{\partial r} = 0, \tag{3.3b}$$

$$u\frac{\partial w'}{\partial r} + w'\frac{\partial w'}{\partial z'} = -\frac{1}{\rho}\frac{\partial p}{\partial z'} + Pr\,\frac{1}{\rho}\frac{1}{r}\frac{\partial}{\partial r}\left(r\mu\frac{\partial w'}{\partial r}\right), \tag{3.3c}$$

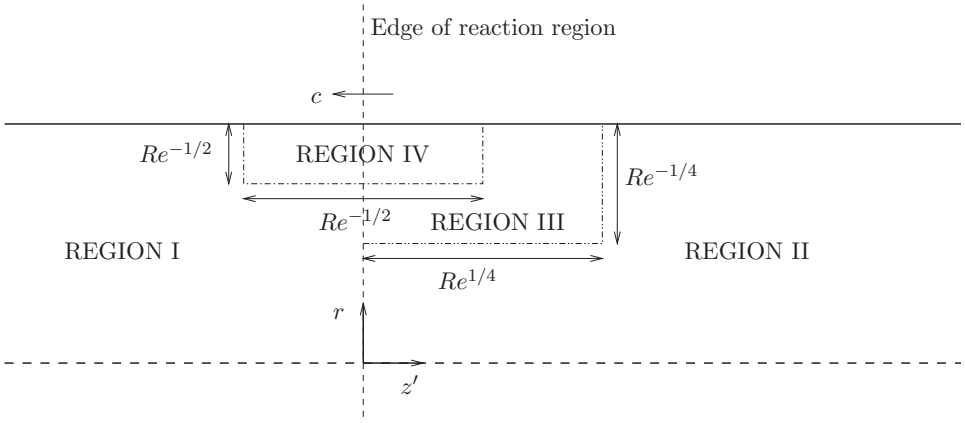


FIGURE 4. Sketch of the tube showing the asymptotic regions.

$$\rho\left(u\frac{\partial T}{\partial r}+w'\frac{\partial T}{\partial z'}\right)=\frac{1}{r}\frac{\partial}{\partial r}\left(rk\frac{\partial T}{\partial r}\right), \tag{3.3$d$}$$

$$\rho T=1, \tag{3.3$e$}$$

at leading order. Taking $Da\to\infty$ in the heat flux boundary condition at $r=1$, (3.2), we have simply $\partial T/\partial r=0$ for $z'<0$ and $T=1+Q$ for $z'>0$. The equations to be solved in the inner two regions can be found by rescaling (3.1).

We construct a region around the edge of the reaction front in which changes in the heat flux due to the reaction are of $O(1)$. The radial scale is therefore determined by considering the heat flux boundary condition at the wall, (3.2). Writing $r^2=1-\eta\bar{R}$ and substituting into (3.2), we have a balance of leading order terms when $\eta=Da^{-1}$. Before we can determine the axial scaling of the inner region we need to know the magnitude of the wave speed. We can determine this by considering the solution in the inlet region and how it matches to the inner region.

### 3.1. *Solution in the inlet region, Region I*

No chemical reaction takes place in region I, and the inlet conditions show that $T=1$, $\rho=1$, $\mu=1$ and $k=1$. The inlet flow is Poiseuille, with $u=0$ and $w'=2\left(1-r^2\right)+c$. From experiments we know that the wave speed is much less than the flow speed, so we write $c=\xi C$ where $\xi\ll 1$ and $C=O(1)$ which gives

$$w'=2\left(1-r^2\right)+\xi C.$$

To obtain the richest balance of terms in the governing equations, we rescale the axial velocity so that it appears at leading order in the innermost asymptotic region. Let $\bar{W}$ be the axial velocity in the inner region so that $w'=\xi\left(\bar{W}+C\right)$. In terms of the region IV scaled variable $\bar{R}$, we obtain

$$\bar{W}=2\xi^{-1}Da^{-1}\bar{R},$$

so the richest balance occurs when $\xi=Da^{-1}$. This allows us to determine the equations in region IV.

### 3.2. *Equations in region IV*

We write $r^2 = 1 - Da^{-1}\bar{R}$, $z' = Da^{-3}\bar{Z}$, $w' = Da^{-1}\left(\bar{W} + C\right)$ and substitute into (3.1). At leading order we obtain

$$\frac{\partial}{\partial \bar{R}}\left(\rho \bar{U}\right) + \frac{\partial}{\partial \bar{Z}}\left(\rho(\bar{W} + C)\right) = 0, \tag{3.4a}$$

$$\frac{1}{2}\bar{U}\frac{\partial \bar{U}}{\partial \bar{R}} + \frac{1}{2}(\bar{W} + C)\frac{\partial \bar{U}}{\partial \bar{Z}} = -\bar{q}^2\frac{2}{\rho}\frac{\partial \bar{P}}{\partial \bar{R}} + \frac{Pr}{3\rho}\left[8\frac{\partial}{\partial \bar{R}}\left(\mu\frac{\partial \bar{U}}{\partial \bar{R}}\right) + 6\frac{\partial}{\partial \bar{Z}}\left(\mu\frac{\partial \bar{W}}{\partial \bar{R}}\right) - 4\frac{\partial}{\partial \bar{R}}\left(\mu\frac{\partial \bar{W}}{\partial \bar{Z}}\right)\right] + \frac{Pr}{\bar{q}^2}\frac{1}{2\rho}\frac{\partial}{\partial \bar{Z}}\left(\mu\frac{\partial \bar{U}}{\partial \bar{Z}}\right), \tag{3.4b}$$

$$\bar{U}\frac{\partial \bar{W}}{\partial \bar{R}} + (\bar{W} + C)\frac{\partial \bar{W}}{\partial \bar{Z}} = -\frac{1}{\rho}\frac{\partial \bar{P}}{\partial \bar{Z}} + \frac{1}{\bar{q}^2}\frac{Pr}{3\rho}\left[3\frac{\partial}{\partial \bar{R}}\left(\mu\frac{\partial \bar{U}}{\partial \bar{Z}}\right) - 2\frac{\partial}{\partial \bar{Z}}\left(\mu\frac{\partial \bar{U}}{\partial \bar{R}}\right) + 4\frac{\partial}{\partial \bar{Z}}\left(\mu\frac{\partial \bar{W}}{\partial \bar{Z}}\right)\right] + \frac{4Pr}{\rho}\frac{\partial}{\partial \bar{R}}\left(\mu\frac{\partial \bar{W}}{\partial \bar{R}}\right), \tag{3.4c}$$

$$\rho\bar{U}\frac{\partial T}{\partial \bar{R}} + \rho\left(\bar{W} + C\right)\frac{\partial T}{\partial \bar{Z}} = 4\frac{\partial}{\partial \bar{R}}\left(k\frac{\partial T}{\partial \bar{R}}\right) + \frac{1}{\bar{q}^2}\frac{\partial}{\partial \bar{Z}}\left(k\frac{\partial T}{\partial \bar{Z}}\right), \tag{3.4d}$$

$$\rho T = 1, \tag{3.4e}$$

where $\bar{U} = -2Da^{-1}u$. The rescaled pressure, $\bar{P}$, is given by $p = Da^{-2}\bar{P}$, where $p$ is the pressure in the outer regions. The parameter $\bar{q}$ is given by $\bar{q} = qDa^{-2}$, and we assume that $\bar{q} = O(1)$.

The boundary conditions in region IV are

$$\bar{U} = 0, \quad \bar{W} = 0, \quad k\frac{\partial T}{\partial \bar{R}} = \begin{cases} \frac{1}{2}\rho\left(T - 1 - Q\right), & \bar{Z} > 0, \\ 0, & \bar{Z} < 0, \end{cases} \quad \text{at } \bar{R} = 0, \tag{3.5a}$$

$$\bar{U} \to 0, \quad \bar{W} \sim 2\bar{R}, \quad T \to 1 \quad \text{as } \bar{Z} \to -\infty, \tag{3.5b}$$

along with matching to the outer solution as $\bar{R}$, $\bar{Z} \to \infty$. We can now determine the scalings for the intermediate region, III.

### 3.3. *Equations in region III*

Region III is situated between regions II and IV as shown in Figure 4. We rescale using $r^2 = 1 - Da^{-1/2}R$, $z' = Da^{-3/2}Z$ and $w' = Da^{-1/2}W + Da^{-1}C$. Substituting into (3.1), we find the leading order equations to be

$$\frac{\partial}{\partial R}\left(\rho U\right) + \frac{\partial}{\partial Z}\left(\rho W\right) = 0, \tag{3.6a}$$

$$\frac{\partial P}{\partial R} = 0, \tag{3.6b}$$

$$U\frac{\partial W}{\partial R} + W\frac{\partial W}{\partial Z} = -\frac{1}{\rho}\frac{\partial P}{\partial Z} + \frac{4Pr}{\rho}\frac{\partial}{\partial R}\left(\mu\frac{\partial W}{\partial R}\right), \tag{3.6c}$$

$$\rho U\frac{\partial T}{\partial R} + \rho W\frac{\partial T}{\partial Z} = 4\frac{\partial}{\partial R}\left(k\frac{\partial T}{\partial R}\right), \tag{3.6d}$$

$$\rho T = 1. \tag{3.6e}$$

The rescaled pressure, $P$, is given by $p = Da^{-1}P$ and the radial velocity is, $U = -2Da^{-1/2}u$. The boundary conditions at the wall are

$$U = 0, \quad W = 0, \quad T = 1 + Q \quad \text{at } R = 0, \tag{3.7}$$

along with matching to the outer regions as $Z \to 0$ and $R \to \infty$.

We are now in a position to solve the systems of equations we have obtained in each of the asymptotic regions. We have already described the simple solution in region I, the inlet region, in Section 3.1. We will consider the solution in the three other regions for two different cases. The more complicated of the two is the $O(1)$ heat release problem, which is given by the fully compressible equations. In order to gain some insight, we first consider the case of small heat release, which is significantly more straightforward to tackle than the full problem.

## 4. Solution for small heat release

The complexity of the systems to be solved in regions II, III and IV can be reduced by assuming that the heat of reaction, $Q$, is small. This approximation is not very realistic physically, but it simplifies the equations greatly and can be used as a check on the accuracy of our solutions when $Q = O(1)$ in the limit $Q \to 0$. Moreover, the solution for $Q \ll 1$ retains most of the features and physics of the full problem. When $Q \ll 1$, the temperature remains close to its inlet value, so it is appropriate to define $T = 1 + Q\hat{T}$. It follows from the equation of state that, to leading order, the density is also constant (the constant density approximation) and, since the viscosity and thermal conductivity are dependent only on the temperature, we have $\mu = 1$ and $k = 1$ at leading order. Using the constant density approximation, we therefore find that the flow down the tube is unchanged, with $u = 0$ and $w' = 2(1-r^2)+Da^{-1}C$ at leading order. The energy equation is now the only nontrivial equation to be solved. In each of the asymptotic regions, the leading order equation can be found by substituting $u = 0$, $w' = 2(1 - r^2) + Da^{-1}C$, $T = 1+Q\hat{T}$, $k = 1$ and $\rho = 1$ into (3.3d), (3.4d) and (3.6d) and their respective boundary conditions.

### 4.1. *Region II*

In this region we have a parabolic governing equation

$$2\left(1 - r^2\right)\frac{\partial \hat{T}}{\partial z'} = \frac{1}{r}\frac{\partial}{\partial r}\left(r\frac{\partial \hat{T}}{\partial r}\right), \tag{4.1}$$

for $0 \leqslant r \leqslant 1$, $0 \leqslant z' < \infty$, to be solved subject to the boundary conditions

$$\frac{\partial \hat{T}}{\partial r} = 0, \qquad \text{at} \quad r = 0, \tag{4.2a}$$

$$\hat{T} = 1, \qquad \text{at} \quad r = 1, \tag{4.2b}$$

$$\hat{T} = 0, \qquad \text{at} \quad z' = 0. \tag{4.2c}$$

We have replaced the requirement that $\hat{T}$ should be finite at $r = 0$ by the equivalent symmetry condition, (4.2a), since we solve this system numerically.

Using a forward stepping, implicit finite difference scheme, we discretise the equations on an $m \times n$ grid, and write the problem in the form

$$A_j\, T_j = B_j\, T_{j-1},$$

where $A_j$ and $B_j$ are known $m \times m$ matrices, $T_j$ is a vector of length $m$ that contains

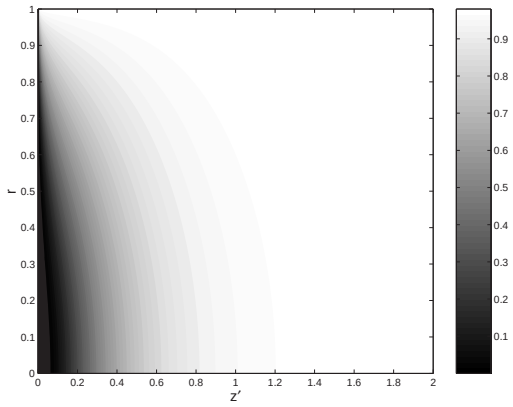


FIGURE 5. Temperature profiles in region II.

the discretized temperature, and $0 \leqslant j \leqslant n$. Writing $T_j = T_g + \Delta T$ where $T_g$ is an approximation to the solution, $T_j$, and $\Delta T$ is a small correction to this, we obtain an equation for $\Delta T$ of the form

$$M_j \Delta T = r_j, \tag{4.3}$$

where $M_j$ is another known $m \times m$ matrix and $r_j$ is a known vector of length $m$. Both $M_j$ and $r_j$ contain the approximate solution $T_g$. We solve (4.3) for $\Delta T$ and use an iterative procedure to improve the approximation for $T_j$ until $\Delta T$ has converged to zero. The numerical solution is shown in Figure 5. The qualitative form of the solution is as we might expect, with the temperature decreasing with distance from the wall and increasing as the distance from the edge of the reaction front, $z'$, increases.

### 4.2. *Region III*

In region III the velocities are $U = 0$ and $W = 2R$. Substituting for $U$, $W$, $k$ and $T$ into (3.6d) we obtain

$$R\frac{\partial \hat{T}}{\partial Z} = 2\frac{\partial^2 \hat{T}}{\partial R^2}, \tag{4.4}$$

where $0 \leqslant R < \infty$, $0 \leqslant Z < \infty$, with the boundary conditions

$$\hat{T} = 1, \qquad \text{at} \quad R = 0, \tag{4.5a}$$

$$\hat{T} \to 0, \qquad \text{as} \quad R \to \infty, \tag{4.5b}$$

$$\hat{T} = 0, \qquad \text{at} \quad Z = 0. \tag{4.5c}$$

We obtained the boundary condition as $R \to \infty$ by matching to the outer solution in region II where $\hat{T} \to 0$ as $z' \to 0$. By looking for a similarity solution of the form $\hat{T}\left(R/(3Z)^{1/3}\right)$ we find the solution to be

$$\hat{T} = 1 - P\left(\frac{1}{3}, \frac{R^3}{18Z}\right), \tag{4.6}$$

where $P$ is the incomplete gamma function defined by

$$P(a, x) = \frac{1}{\Gamma(a)} \int_0^x e^{-t} t^{a-1} \, \mathrm{d}t.$$

This solution is shown in Figure 6.

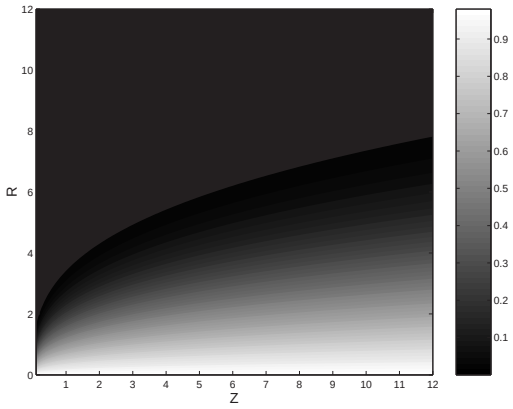


FIGURE 6. Temperature in region III.

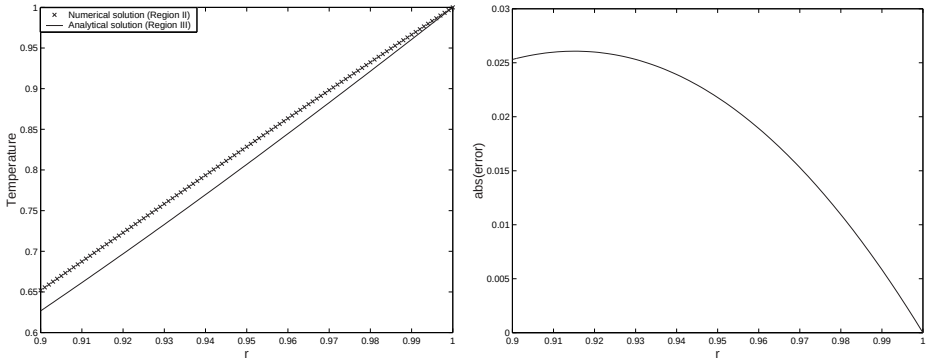


(a) Solutions from regions II and III at $z' = 0.01$ (b) Error between matched solutions

FIGURE 7. Comparison of results in regions II and III.

### 4.3. *Matching between regions II and III*

In order to confirm that the solutions in regions II and III match, we write the solution in region III, (4.6), in terms of the variables of region II to give

$$\hat{T} = 1 - P\left(\frac{1}{3}, \frac{(1-r^2)^3}{18z'}\right).$$

The region II solution should match with this as $r \to 1$, $z' \to 0$. The comparison between the two solutions is shown in Figure 7. The two solutions match relatively closely, with a maximum absolute error of around 2.5%, see Figure 7. The matching can be improved by calculating a correction to the solution in region III. We will not give the details here (see Adamson 2004), but find that the corrected matching condition in region II is

$$\hat{T} \sim 1 - P\left(\frac{1}{3}, \frac{(1-r^2)^3}{18z'}\right) + \frac{(1-r^2)}{5} P\left(\frac{4}{3}, \frac{(1-r^2)^3}{18z'}\right) - \frac{(1-r^2)}{2} P\left(\frac{1}{3}, \frac{(1-r^2)^3}{18z'}\right) + \frac{3}{10}(1-r^2) \quad \text{as } r \to 1,\ z' \to 0. \tag{4.7}$$

Figure 8 shows that the matching between solutions has been greatly improved by adding this correction term. We move on to investigate the solution in the innermost region,

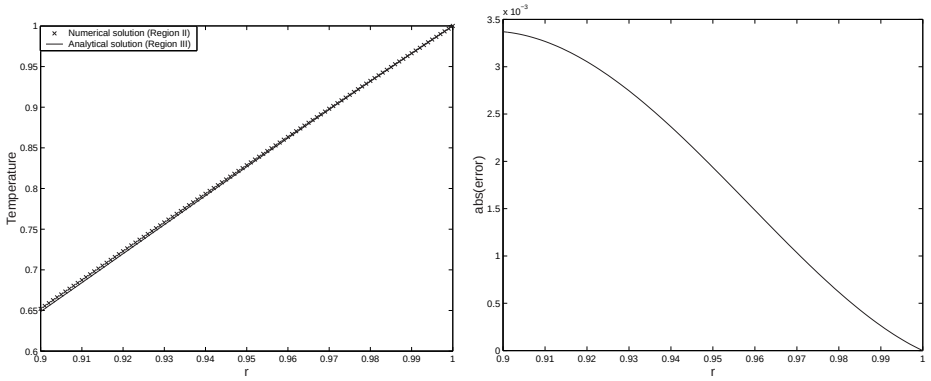


(a) Solutions from regions II and III at $z' = 0.01$ (b) Error between matched solutions

FIGURE 8. Matching with corrected region III solution.

region IV, where matching with the solution in region III provides the boundary condition for large $\bar{R}$ and $\bar{Z}$.

### 4.4. *Region IV*

The velocities in region IV are $\bar{U} = 0$ and $\bar{W} = 2\bar{R}$. Substituting for $\bar{U}$, $\bar{W}$, $k$ and $T$ into (3.4d) gives the elliptic governing equation

$$(2\bar{R} + C)\frac{\partial \hat{T}}{\partial \bar{Z}} = 4\frac{\partial^2 \hat{T}}{\partial \bar{R}^2} + \frac{1}{\bar{q}^2}\frac{\partial^2 \hat{T}}{\partial \bar{Z}^2}, \tag{4.8}$$

for $0 \leqslant \bar{R} < \infty$, $-\infty < \bar{Z} < \infty$, which we solve subject to the conditions

$$\frac{\partial \hat{T}}{\partial \bar{R}} = \begin{cases} \frac{1}{2}\left(\hat{T} - 1\right), & \bar{Z} > 0, \\ 0, & \bar{Z} < 0, \end{cases} \qquad \text{at} \quad \bar{R} = 0, \tag{4.9a}$$

$$\hat{T} \to 0, \qquad \text{as} \quad \bar{Z} \to -\infty, \tag{4.9b}$$

$$\hat{T} \to \text{Region III solution}, \qquad \text{as} \quad \bar{R},\, \bar{Z} \to \infty. \tag{4.9c}$$

Since we wish to solve this system numerically, we must smooth the discontinuous boundary condition at $\bar{R} = 0$ to reduce errors close to $\bar{Z} = 0$. We replace the Heaviside function with a hyperbolic tangent giving

$$\frac{\partial \hat{T}}{\partial \bar{R}} = \frac{1}{4}\left(\hat{T} - 1\right)\left\{1 + \tanh(\delta^{-1}\bar{Z})\right\},$$

where $\delta$ is a small parameter of the order of the step size in $\bar{Z}$. The matching conditions as $\bar{R} \to \infty$† and $\bar{Z} \to \infty$ are given by the corrected region III solution, (4.7), written in

† For $\bar{Z} < 0$ the condition as $\bar{R} \to \infty$ is that $\hat{T} \to 0$, since for small $\bar{Z}$ we have $\hat{T} \to 0$ and $\hat{T} = 0$ in the inlet region.

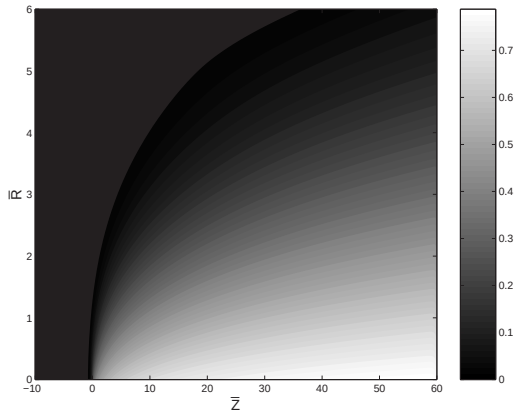


FIGURE 9. Solution in region IV.

terms of the region IV variables as

$$\hat{T}(\bar{R},\bar{Z}) \sim 1 - P\left(\frac{1}{3},\frac{\bar{R}^3}{18\bar{Z}}\right) + \frac{3}{8\pi^2}2^{1/6}\Gamma(5/6)\Gamma(2/3)(C-4)\frac{1}{(3Z)^{1/3}}\sqrt{\frac{R}{(3Z)^{1/3}}}K_{1/6}\left(\frac{R^3}{36Z}\right)\exp\left(-\frac{R^3}{36Z}\right) - \frac{3C}{2\Gamma(1/3)}\frac{1}{6^{1/3}}\frac{1}{(3Z)^{1/3}}\exp\left(-\frac{R^3}{18Z}\right).$$

We solve numerically, with the temperature given by an array with components, $T_{i,\,j}$, representing the temperature at $\bar{R}_i$, $\bar{Z}_j$ on a uniform grid of $m \times n$ points. We truncate the semi-infinite range in $\bar{R}$ and infinite range in $\bar{Z}$ so that $0 \leqslant \bar{R}_j \leqslant 10$ and $-10 \leqslant \bar{Z}_j \leqslant 60$. We calculate the derivatives of the discrete function $T_{i,\,j}$ using a five point centred difference formula in the bulk and a four point biassed stencil formulae at the edges of the solution grid. In discrete form, (4.8) is given by

$$a_j\mathbf{T}_{j+2} + b_j\mathbf{T}_{j+1} + c_j\mathbf{T}_j + d_j\mathbf{T}_{j-1} + e_j\mathbf{T}_{j-2} = \mathbf{r}_j,$$

where $a_j$, $b_j$, $c_j$, $d_j$ and $e_j$ are $m \times m$ arrays and $\mathbf{T}_j(= T_{i,\,j})$ and $\mathbf{r}_j$ are vectors of length $m$. We solved this system using a Thomas algorithm (Fletcher 1991).

When we tested the numerical solution for mesh dependence, we found that the largest errors occur around $\bar{R} = 0$, $\bar{Z} = 0$, where the change in heat flux is maximum, but that these errors decrease as the grid spacing in $\bar{R}$ and $\bar{Z}$ is reduced. To minimise errors, without making the computational time too great, we chose grid spacings of 0.1. A plot of the temperature, $\hat{T}$, for $C = 1.0$ is shown in Figure 9. Although we made use of the corrected region III solution in our boundary conditions, the region IV solution does not tend smoothly to the matching condition as $\bar{Z} \to \infty$. To correct this, we calculated the next order solution in region III. After much algebra (Adamson 2004) we found the

$O(Da^{-1})$ solution

$$\hat{T}_2 = \frac{1}{(3Z)^{2/3}}\left[B_1 \exp\left(-\frac{R^3}{18Z}\right)\right.$$
$$-\frac{CA_1}{8}\exp\left(-\frac{R^3}{36Z}\right)\left(\frac{R}{(3Z)^{1/3}}\right)^{5/2}\left[K_{1/6}\left(\frac{R^3}{36Z}\right)+K_{5/6}\left(\frac{R^3}{36Z}\right)\right]$$
$$\left.+\frac{CA_2}{8}\left(\frac{R}{(3Z)^{1/3}}\right)^{2}\exp\left(-\frac{R^3}{18Z}\right)\right],$$

where

$$B_1 = \frac{2^{1/6}\,24^{5/6}\,3}{128\pi^2}\Gamma(2/3)\left(\Gamma(5/6)\right)^2(C-4)^2.$$

When this is written in terms of the region IV variables we obtain the same expression but with $\bar{R}$ and $\bar{Z}$ in place of $R$ and $Z$, and the whole expression is of $O(Da)$. Hence we find that $\hat{T}_2$ appears at leading order in the correction to the matching condition between regions III and IV. We solved the system described by (4.8) and the boundary conditions, (4.9), with this new matching condition and obtained the following results.

#### 4.4.1. *Variation of wave speed with critical temperature*

We obtained results at different values of the wave speed, $C$, for $\bar{q} = 1$, as shown in Figure 10. Comparing these solutions we find that for small $C$ the temperature increases more rapidly than for large $C$ so that, at a given point, the temperature is greater when the wave speed is smaller. We obtained results at several wave speeds and for each value of $C$ noted the temperature at $\bar{R} = 0$, $\bar{Z} = 0$, which is the critical temperature, $\hat{T}_c$, to which the solution corresponds. A plot, which shows that the wave speed decreases with critical temperature, is shown in Figure 11.

#### 4.4.2. *Variation of wave speed with mass flow rate*

Taking a fixed value of critical temperature we varied $\bar{q}$ to determine the effect on the wave speed. The results for $\hat{T}_c = 0.2$ are shown in Figure 12. Increasing the mass flow rate causes the wave speed to decrease, and reach zero at $\bar{q} \approx 2.48$. For $\bar{q} > 2.48$ the wave speed is negative so that, instead of propagating towards the inlet of the tube, the wave front moves towards the outlet and will eventually be blown out.

The solution for small $Q$ shows that the flame speed depends on both the mass flow rate of fuel into the tube and the critical temperature at which the reaction starts, $\hat{T}_c$. The latter is related to the amount of catalyst present on the inner surface of the tube; the more catalyst present the lower $\hat{T}_c$ will be. These effects could both be tested experimentally. We make a comparison with experiment in Section 6, but first we tackle the problem when $Q = O(1)$.

## 5. Solution for $O(1)$ heat release

When $Q = O(1)$, the solution in the inlet region, which we discussed in Section 3.1, remains unchanged. In the other three regions, however, we must solve the more complicated system of fully compressible equations.

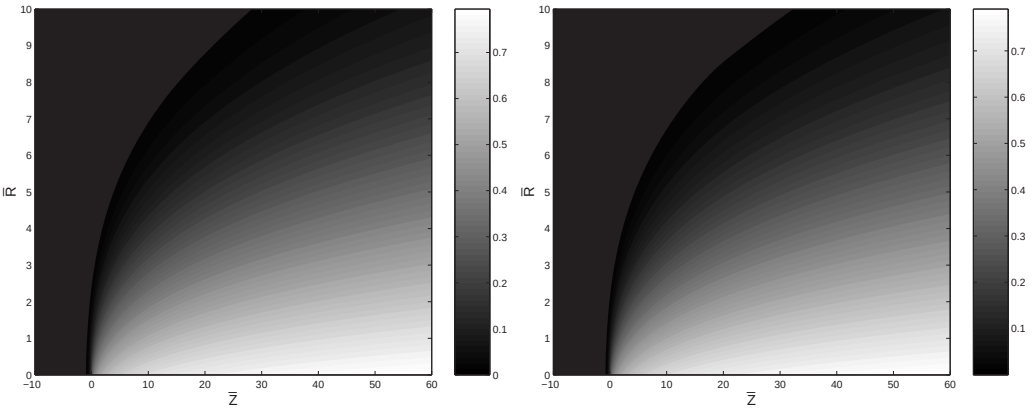


(a) $C = 0.5$ (b) $C = 1.0$

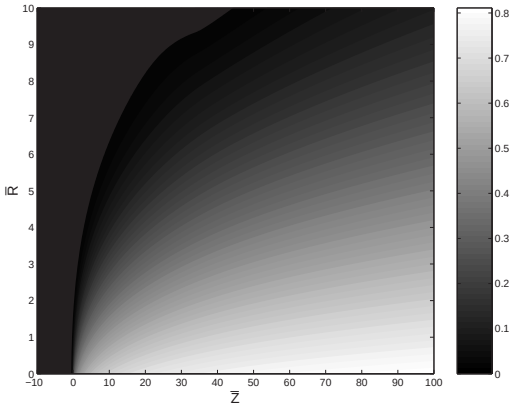


(c) $C = 2.0$

FIGURE 10. Solutions in region IV.

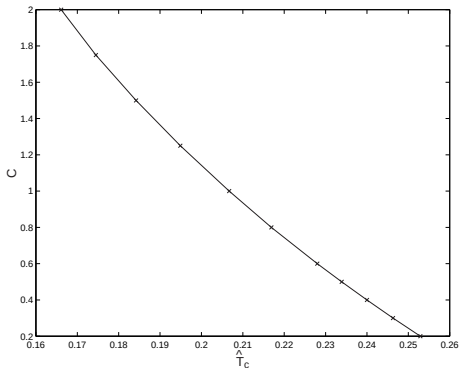


FIGURE 11. Plot of wave speed, $C$, against critical temperature, $\hat{T}_c$.

### 5.1. *Region II*

In this region we solve (3.3) subject to the boundary conditions

$$u = 0, \qquad w' = 0, \qquad T = 1 + Q, \qquad \text{at} \qquad r = 1, \tag{5.1a}$$

$$u = 0, \qquad w' = 2\left(1 - r^2\right), \qquad T = 1, \qquad \text{at} \qquad z' = 0. \tag{5.1b}$$

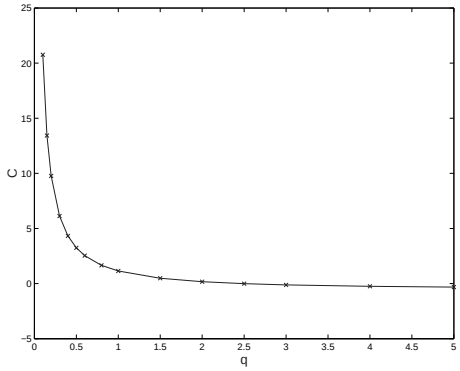


FIGURE 12. Plot of wave speed, $C$, against mass flow rate of fuel, $\bar{q}$.

We also require that $u$, $w'$ and $T$ are finite at $r = 0$. We assume that the fluid behaves like the model fluid described by Stewartson (1964), so that the Prandtl number, $Pr = 1$, and the viscosity and thermal conductivity are directly proportional to temperature, $\mu = T$, $k = T$. In terms of the streamfunction, $\psi$, defined by

$$\frac{\partial \psi}{\partial z'} = r\rho u, \qquad \frac{\partial \psi}{\partial r} = -r\rho w',$$

so that conservation of mass, (3.3a), is satisfied, (3.3)(c) and (d) become

$$\begin{aligned}
&-3\frac{T}{r^4}\frac{\partial\psi}{\partial z'}\frac{\partial\psi}{\partial r} - \frac{T}{r^3}\frac{\partial\psi}{\partial r}\frac{\partial^2\psi}{\partial r\partial z'} + \frac{3}{r^3}\frac{\partial T}{\partial r}\frac{\partial\psi}{\partial z'}\frac{\partial\psi}{\partial r} + 3\frac{T}{r^3}\frac{\partial\psi}{\partial z'}\frac{\partial^2\psi}{\partial r^2} - \frac{1}{r^2}\frac{\partial^2 T}{\partial r^2}\frac{\partial\psi}{\partial z'}\frac{\partial\psi}{\partial r} \\
&\quad - \frac{2}{r^2}\frac{\partial T}{\partial r}\frac{\partial\psi}{\partial z'}\frac{\partial^2\psi}{\partial r^2} - \frac{T}{r^2}\frac{\partial\psi}{\partial z'}\frac{\partial^3\psi}{\partial r^3} - \frac{2}{r^3}\frac{\partial T}{\partial z'}\left(\frac{\partial\psi}{\partial r}\right)^2 + \frac{2}{r^2}\frac{\partial T}{\partial z'}\frac{\partial^2\psi}{\partial r^2}\frac{\partial\psi}{\partial r} \\
&\quad + \frac{1}{r^2}\frac{\partial^2 T}{\partial r\partial z'}\left(\frac{\partial\psi}{\partial r}\right)^2 + \frac{T}{r^2}\frac{\partial\psi}{\partial r}\frac{\partial^3\psi}{\partial z'\partial r^2} = 3\frac{T^2}{r^4}\frac{\partial\psi}{\partial r} - 6\frac{T}{r^3}\frac{\partial T}{\partial r}\frac{\partial\psi}{\partial r} - 3\frac{T^2}{r^3}\frac{\partial^2\psi}{\partial r^2} \\
&\quad + \frac{3}{r^2}\left(\frac{\partial T}{\partial r}\right)^2\frac{\partial\psi}{\partial r} + 7\frac{T}{r^2}\frac{\partial T}{\partial r}\frac{\partial^2\psi}{\partial r^2} + 2\frac{T^2}{r^2}\frac{\partial^3\psi}{\partial r^3} + 3\frac{T}{r^2}\frac{\partial^2 T}{\partial r^2}\frac{\partial\psi}{\partial r} - \frac{3}{r}\frac{\partial T}{\partial r}\frac{\partial^2 T}{\partial r^2}\frac{\partial\psi}{\partial r} \\
&\quad - \frac{4}{r}\left(\frac{\partial T}{\partial r}\right)^2\frac{\partial^2\psi}{\partial r^2} - \frac{T}{r}\frac{\partial^3 T}{\partial r^3}\frac{\partial\psi}{\partial r} - 4\frac{T}{r}\frac{\partial^2 T}{\partial r^2}\frac{\partial^2\psi}{\partial r^2} - 5\frac{T}{r}\frac{\partial T}{\partial r}\frac{\partial^3\psi}{\partial r^3} - \frac{T^2}{r}\frac{\partial^4\psi}{\partial r^4}, \qquad (5.2a)
\end{aligned}$$

$$\frac{\partial\psi}{\partial z'}\frac{\partial T}{\partial r} - \frac{\partial\psi}{\partial r}\frac{\partial T}{\partial z'} = T\frac{\partial T}{\partial r} + r\left(\frac{\partial T}{\partial r}\right)^2 + rT\frac{\partial^2 T}{\partial r^2}, \qquad (5.2b)$$

where we have used the fact that $\partial p/\partial r = 0$ to remove the pressure terms. The boundary conditions for $\psi$ and $T$ are

$$\psi = -\frac{1}{2}, \qquad \frac{\partial\psi}{\partial r} = 0, \qquad T = 1 + Q, \qquad \text{at} \qquad r = 1, \qquad (5.3a)$$

$$\psi = -\left(r^2 - \frac{r^4}{2}\right), \qquad \frac{\partial\psi}{\partial z'} = 0, \qquad T = 1, \qquad \text{at} \qquad z' = 0. \qquad (5.3b)$$

As $u$ and $w'$ must be finite at $r = 0$ we require that

$$\psi = 0, \qquad \frac{\partial\psi}{\partial r} = 0,$$

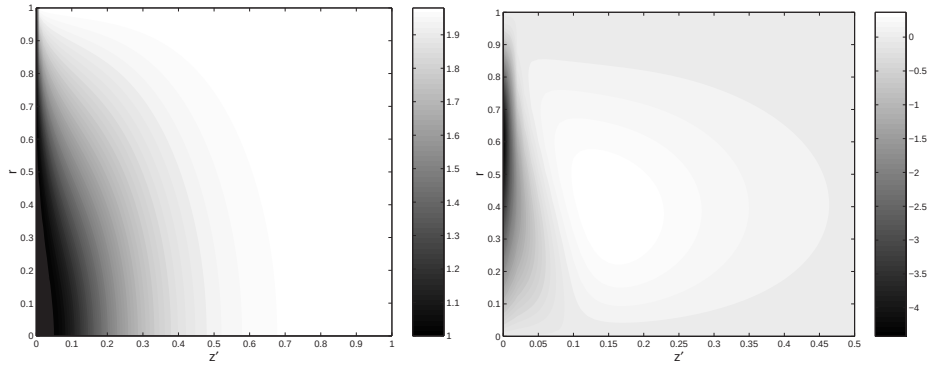


(a) Temperature (b) Radial velocity

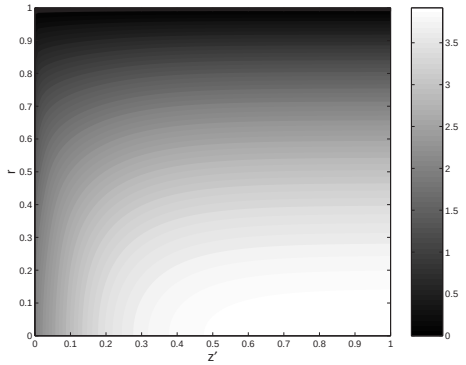


(c) Axial velocity

FIGURE 13. Solutions in region II.

and also impose the symmetry condition

$$\frac{\partial T}{\partial r} = 0, \qquad \text{at} \quad r = 0.$$

We solved this system using a numerical scheme that follows the basic principles of the method described in Section 4.1. The process is more complicated, however, as we now solve two equations simultaneously. Some typical solutions are shown in Figure 13.

The temperature profiles are qualitatively similar to those we obtained when $Q \ll 1$. The axial velocity increases most quickly close to the wall of the tube where the temperature is highest. As $z'$ becomes large the velocity field tends to a steady Poiseuille profile again, but the maximum velocity here is larger than it was in the inlet region, because of the expansion of the heated gas. The radial velocity increases quickly at small $z'$ as the heated fluid moves away from the wall. In fact, the solution for $u$ jumps from zero at $z' = 0$ to a large negative value at the first calculated value of $z'$. The magnitude of this jump increases as the step size in $z'$ is decreased so that as $z' \to 0$ there appears to be a singularity in the radial velocity solution. There are no physical singularities in our problem, which suggests that as $z' \to 0$ the solution in region II becomes nonuniform. Our asymptotic structure should include another region which smoothes out the solution for small $z'$. Figure 14 shows the new asymptotic structure where extra regions, IIa and IIIa, have been added around the reaction front. Region III is drawn as a boundary layer to show more easily how the regions match together. Regions IIa and IIIa match

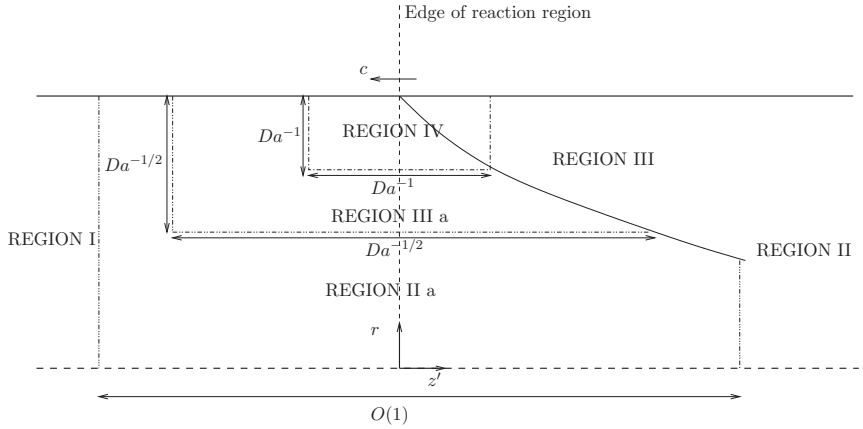


FIGURE 14. Sketch of the tube showing the additional asymptotic regions.

the solutions of regions I and II when $r = O(1)$ and $r = O(Da^{-1/2})$ respectively. We describe the solution in these two new regions in the appendix.

### 5.2. *Region III*

In this region, we solve (3.6) subject to the boundary conditions

$$U = 0, \quad W = 0, \quad T = 1 + Q, \qquad \text{at } R = 0, \tag{5.4a}$$

$$U,\ W,\ T \sim \text{Region IIIa solution}, \qquad \text{as } R \to \infty,\ Z \to 0. \tag{5.4b}$$

When written in terms of the region III variables, the region IIIa solutions are, to leading order,

$$T = 1 + Da^{-\gamma} \exp\left(-\frac{R^3}{18Z}\right),$$

$$\Psi = R^2 + 2Da^{-\gamma-1} \exp\left(-\frac{R^3}{18Z}\right),$$

where $\Psi = Da\left(2\psi + 1 + Da^{-1}C\right)$and $\gamma$ is a constant, which can be determined by higher order matching. The streamfunction, $\Psi$, is related to the velocities, $U$ and $W$, by

$$\frac{\partial \Psi}{\partial R} = \rho W, \qquad \frac{\partial \Psi}{\partial Z} = -\rho U,$$

so conservation of mass, (3.6a), is satisfied. We look for a similarity solution of the form

$$T = T(\eta), \qquad \Psi = (3Z)^{2/3} f(\eta), \qquad \text{where} \qquad \eta = \frac{R}{(3Z)^{1/3}}.$$

After removing the pressure terms from the momentum equations, by differentiating (3.6c) with respect to $R$, we obtain the governing equations in terms of $T$ and $f$ as

$$-2f\frac{\mathrm{d}f}{\mathrm{d}\eta}\frac{\mathrm{d}^2T}{\mathrm{d}\eta^2} - 4f\frac{\mathrm{d}^2f}{\mathrm{d}\eta^2}\frac{\mathrm{d}T}{\mathrm{d}\eta} - 2f\frac{\mathrm{d}^3f}{\mathrm{d}\eta^3}T - \left(\frac{\mathrm{d}f}{\mathrm{d}\eta}\right)^2\frac{\mathrm{d}T}{\mathrm{d}\eta} = 12\frac{\mathrm{d}T}{\mathrm{d}\eta}\frac{\mathrm{d}^2T}{\mathrm{d}\eta^2}\frac{\mathrm{d}f}{\mathrm{d}\eta}$$
$$+16\left(\frac{\mathrm{d}T}{\mathrm{d}\eta}\right)^2\frac{\mathrm{d}^2f}{\mathrm{d}\eta^2} + 4T\frac{\mathrm{d}^3T}{\mathrm{d}\eta^3}\frac{\mathrm{d}f}{\mathrm{d}\eta} + 16T\frac{\mathrm{d}^2T}{\mathrm{d}\eta^2}\frac{\mathrm{d}^2f}{\mathrm{d}\eta^2} + 20T\frac{\mathrm{d}T}{\mathrm{d}\eta}\frac{\mathrm{d}^3f}{\mathrm{d}\eta^3} + 4T^2\frac{\mathrm{d}^4f}{\mathrm{d}\eta^4}, \tag{5.5a}$$

$$4\left(\frac{\mathrm{d}T}{\mathrm{d}\eta}\right)^2 + 4T\frac{\mathrm{d}^2T}{\mathrm{d}\eta^2} + 2f\frac{\mathrm{d}T}{\mathrm{d}\eta} = 0. \tag{5.5b}$$

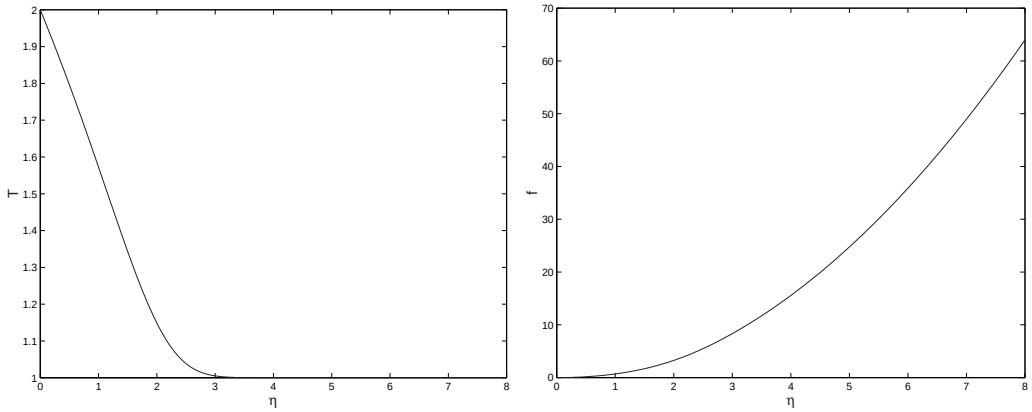


(a) Temperature (b) Stream function

FIGURE 15. Solutions in region III.

The boundary conditions at the wall, $\eta = 0$, are

$$f = 0, \qquad \frac{\mathrm{d}f}{\mathrm{d}\eta} = 0, \qquad T = 1 + Q, \tag{5.6}$$

and as $\eta \to \infty$ we have

$$T \sim 1 + Da^{-\gamma} \exp\left(-\frac{\eta^3}{6}\right), \tag{5.7a}$$

$$f \sim \eta^2 + \frac{1}{(3Z)^{2/3}} 2Da^{-\gamma-1} \exp\left(-\frac{\eta^3}{6}\right). \tag{5.7b}$$

Although it appears that the boundary condition in (5.7b) is not in similarity form, we can assume that the term in $Z$ in front of the exponential is part of the next order solution in region IIIa, and therefore that

$$f \sim \eta^2 + 2Da^{-\gamma-1} \exp\left(-\frac{\eta^3}{6}\right), \tag{5.8}$$

to leading order. Differentiating (5.7a) and (5.8) and eliminating the exponential terms gives the boundary conditions

$$\begin{aligned} &\frac{\mathrm{d}f}{\mathrm{d}\eta} + \frac{\eta^2}{2} f \sim 2\eta + \frac{\eta^4}{2}, \\ &\frac{\mathrm{d}^2 f}{\mathrm{d}\eta^2} + \frac{\eta^2}{2}\frac{\mathrm{d}f}{\mathrm{d}\eta} + \eta f \sim 2 + 2\eta^3, \qquad \text{as} \qquad \eta \to \infty. \\ &\frac{\mathrm{d}T}{\mathrm{d}\eta} + \frac{\eta^2}{2} T \sim \frac{\eta^2}{2}, \end{aligned}$$

We solved (5.5) numerically using a finite difference scheme and the solutions, when $Q = 1$, are shown in Figure 15.

### 5.3. *Region IV*

The equations to be solved in this region are (3.4) with the boundary conditions, (3.5). Differentiating (3.4b) and (3.4c) with respect to $\bar{Z}$ and $\bar{R}$ respectively, we then combine

them so as to remove the pressure terms. We define the streamfunction, $\bar{\psi}$, using

$$\frac{\partial\bar{\psi}}{\partial\bar{Z}} = -\rho\bar{U}, \qquad \frac{\partial\bar{\psi}}{\partial\bar{R}} = \rho\left(\bar{W}+C\right),$$

and, setting $\mu = T$, $k = T$ as before, we substitute $\bar{\psi}$ and $T$ for $u$, $w'$, $\mu$, $k$ and $\rho$ into the momentum and energy equations giving

$$\begin{aligned}
&-\frac{\partial T}{\partial\bar{R}}\frac{\partial^2\bar{\psi}}{\partial\bar{Z}^2}\frac{\partial\bar{\psi}}{\partial\bar{Z}} - \frac{1}{2}\frac{\partial^2 T}{\partial\bar{R}\partial\bar{Z}}\left(\frac{\partial\bar{\psi}}{\partial\bar{Z}}\right)^2 - \frac{1}{2}T\frac{\partial\bar{\psi}}{\partial\bar{Z}}\frac{\partial^3\bar{\psi}}{\partial\bar{R}\partial\bar{Z}^2} + \frac{1}{2}\frac{\partial^2 T}{\partial\bar{Z}^2}\frac{\partial\bar{\psi}}{\partial\bar{R}}\frac{\partial\bar{\psi}}{\partial\bar{Z}} + \frac{\partial T}{\partial\bar{Z}}\frac{\partial\bar{\psi}}{\partial\bar{R}}\frac{\partial^2\bar{\psi}}{\partial\bar{Z}^2}\\
&\quad+\frac{1}{2}T\frac{\partial\bar{\psi}}{\partial\bar{R}}\frac{\partial^3\bar{\psi}}{\partial\bar{Z}^3} - 2\bar{q}^2\frac{\partial^2 T}{\partial\bar{R}^2}\frac{\partial\bar{\psi}}{\partial\bar{Z}}\frac{\partial\bar{\psi}}{\partial\bar{R}} - 4\bar{q}^2\frac{\partial T}{\partial\bar{R}}\frac{\partial\bar{\psi}}{\partial\bar{Z}}\frac{\partial^2\bar{\psi}}{\partial\bar{R}^2} - 2\bar{q}^2 T\frac{\partial\bar{\psi}}{\partial\bar{Z}}\frac{\partial^3\bar{\psi}}{\partial\bar{R}^3} + 4\bar{q}^2\frac{\partial T}{\partial\bar{Z}}\frac{\partial^2\bar{\psi}}{\partial\bar{R}^2}\frac{\partial\bar{\psi}}{\partial\bar{R}}\\
&\quad+2\bar{q}^2\frac{\partial^2 T}{\partial\bar{R}\partial\bar{Z}}\left(\frac{\partial\bar{\psi}}{\partial\bar{R}}\right)^2 + 2\bar{q}^2 T\frac{\partial\bar{\psi}}{\partial\bar{R}}\frac{\partial^3\bar{\psi}}{\partial\bar{R}^2\partial\bar{Z}} = 4\frac{\partial T}{\partial\bar{R}}\frac{\partial^2 T}{\partial\bar{R}\partial\bar{Z}}\frac{\partial\bar{\psi}}{\partial\bar{Z}} + 2\frac{\partial T}{\partial\bar{Z}}\frac{\partial^2 T}{\partial\bar{R}^2}\frac{\partial\bar{\psi}}{\partial\bar{Z}}\\
&\quad+2T\frac{\partial^3 T}{\partial\bar{R}^2\partial\bar{Z}}\frac{\partial\bar{\psi}}{\partial\bar{Z}} + 16\frac{\partial T}{\partial\bar{Z}}\frac{\partial T}{\partial\bar{R}}\frac{\partial^2\bar{\psi}}{\partial\bar{R}\partial\bar{Z}} + 16T\frac{\partial^2 T}{\partial\bar{R}\partial\bar{Z}}\frac{\partial^2\bar{\psi}}{\partial\bar{R}\partial\bar{Z}} + 10T\frac{\partial T}{\partial\bar{R}}\frac{\partial^3\bar{\psi}}{\partial\bar{R}\partial\bar{Z}^2}\\
&\quad+10T\frac{\partial T}{\partial\bar{Z}}\frac{\partial^3\bar{\psi}}{\partial\bar{R}^2\partial\bar{Z}} + 4T^2\frac{\partial^4\bar{\psi}}{\partial\bar{R}^2\partial\bar{Z}^2} + 4\frac{\partial^2 T}{\partial\bar{R}\partial\bar{Z}}\frac{\partial T}{\partial\bar{Z}}\frac{\partial\bar{\psi}}{\partial\bar{R}} + 2\frac{\partial T}{\partial\bar{R}}\frac{\partial^2 T}{\partial\bar{Z}^2}\frac{\partial\bar{\psi}}{\partial\bar{R}} + 2T\frac{\partial^3 T}{\partial\bar{R}\partial\bar{Z}^2}\frac{\partial\bar{\psi}}{\partial\bar{R}}\\
&\quad+\frac{1}{2\bar{q}^2}\left(3\frac{\partial T}{\partial\bar{Z}}\frac{\partial^2 T}{\partial\bar{Z}^2}\frac{\partial\bar{\psi}}{\partial\bar{Z}} + 4\left(\frac{\partial T}{\partial\bar{Z}}\right)^2\frac{\partial^2\bar{\psi}}{\partial\bar{Z}^2} + T\frac{\partial^3 T}{\partial\bar{Z}^3}\frac{\partial\bar{\psi}}{\partial\bar{Z}} + 4T\frac{\partial^2 T}{\partial\bar{Z}^2}\frac{\partial^2\bar{\psi}}{\partial\bar{Z}^2}\right.\\
&\quad\left.+5T\frac{\partial T}{\partial\bar{Z}}\frac{\partial^3\bar{\psi}}{\partial\bar{Z}^3} + T^2\frac{\partial^4\bar{\psi}}{\partial\bar{Z}^4}\right) + 8\bar{q}^2\left(3\frac{\partial T}{\partial\bar{R}}\frac{\partial^2 T}{\partial\bar{R}^2}\frac{\partial\bar{\psi}}{\partial\bar{R}} + 4\left(\frac{\partial T}{\partial\bar{R}}\right)^2\frac{\partial^2\bar{\psi}}{\partial\bar{R}^2}\right.\\
&\quad\left.+T\frac{\partial^3 T}{\partial\bar{R}^3}\frac{\partial\bar{\psi}}{\partial\bar{R}} + 4T\frac{\partial^2 T}{\partial\bar{R}^2}\frac{\partial^2\bar{\psi}}{\partial\bar{R}^2} + 5T\frac{\partial T}{\partial\bar{R}}\frac{\partial^3\bar{\psi}}{\partial\bar{R}^3} + T^2\frac{\partial^4\bar{\psi}}{\partial\bar{R}^4}\right),
\end{aligned} \tag{5.9a}$$

and

$$-\frac{\partial\bar{\psi}}{\partial\bar{Z}}\frac{\partial T}{\partial\bar{R}} + \frac{\partial\bar{\psi}}{\partial\bar{R}}\frac{\partial T}{\partial\bar{Z}} = 4\left(\frac{\partial T}{\partial\bar{R}}\right)^2 + 4T\frac{\partial^2 T}{\partial\bar{R}^2} + \frac{1}{\bar{q}^2}\left(\frac{\partial T}{\partial\bar{Z}}\right)^2 + \frac{1}{\bar{q}^2}T\frac{\partial^2 T}{\partial\bar{Z}^2}. \tag{5.9b}$$

The boundary conditions become

$$\bar{\psi} = 0, \quad \frac{\partial\bar{\psi}}{\partial\bar{R}} = \frac{C}{T}, \quad T^2\frac{\partial T}{\partial\bar{R}} = \begin{cases}\frac{1}{2}\left(T-1-Q\right), & \bar{Z}>0,\\ 0, & \bar{Z}<0,\end{cases} \quad \text{at } \bar{R}=0, \tag{5.10a}$$

$$\bar{\psi},\ \frac{\partial\bar{\psi}}{\partial\bar{R}},\ T \to \text{Region IIIa solution} \quad \text{as } \bar{R}\to\infty, \tag{5.10b}$$

$$\frac{\partial\bar{\psi}}{\partial\bar{Z}} \to 0, \quad \bar{\psi}\sim C\bar{R}+\bar{R}^2, \quad T\to 1 \quad \text{as } \bar{Z}\to-\infty, \tag{5.10c}$$

$$\bar{\psi},\ \frac{\partial\bar{\psi}}{\partial\bar{Z}},\ T \to \text{Region III solution} \quad \text{as } \bar{Z}\to\infty. \tag{5.10d}$$

As in the small $Q$ problem, we smooth the heat flux boundary condition at $\bar{R}=0$ using a hyperbolic tangent profile,

$$T^2\frac{\partial T}{\partial\bar{R}} = \frac{1}{2}\left(T-1-Q\right)\frac{1}{2}\left[1+\tanh(\delta^{-1}\bar{Z})\right], \qquad \text{at} \quad \bar{R}=0,$$

where $\delta \ll 1$ is of the order of the step size in $\bar{Z}$. We return to the solutions found in regions IIIa and III to obtain boundary conditions as $\bar{R}\to\infty$ and $\bar{Z}\to\infty$ respectively.

5.3.1. *Boundary conditions as* $\bar{R} \to \infty$

The region IIIa solutions are

$$T = 1 + Da^{-\gamma} \exp\left(-Da\,\phi\right),$$
$$\psi = -\frac{1}{2} - Da^{-1}\frac{C}{2} + Da^{-3/2}\frac{CR^*}{2} + Da^{-1}\frac{R^{*2}}{2} + Da^{-\gamma-2}\exp\left(-Da\,\phi\right),$$

where $\phi$ is given by (A 8) and $t$ is a root of (A 7). In terms of the region IV variables $R^* = Da^{-1/2}\bar{R}$ and $Z^* = Da^{-1/2}\bar{Z}$, and $t \equiv t\left(R^*/Z^*\right)$ therefore remains of $O(1)$ when written in terms of $\bar{R}$, $\bar{Z}$. It follows that $\phi = O(Da^{-1})$ and the region IIIa solutions written in terms of the region IV variables are

$$T = 1 + Da^{-\gamma}\exp\left(-\bar{\phi}\right),$$
$$\bar{\psi} = C\bar{R} + \bar{R}^2 + 2Da^{-\gamma}\exp\left(-\bar{\phi}\right),$$

to leading order, where $\bar{\phi} = Da\,\phi$ and $\bar{\psi} = Da^2\left(2\psi + 1 + Da^{-1}C\right)$. Differentiating these expressions and eliminating exponential terms we obtain

$$\frac{\partial T}{\partial \bar{R}} + \frac{\partial \bar{\phi}}{\partial \bar{R}}T \sim \frac{\partial \bar{\phi}}{\partial \bar{R}},$$
$$\frac{\partial \bar{\psi}}{\partial \bar{R}} + \frac{\partial \bar{\phi}}{\partial \bar{R}}\bar{\psi} \sim C + 2\bar{R} + \left(C\bar{R} + \bar{R}^2\right)\frac{\partial \bar{\phi}}{\partial \bar{R}},$$
$$\frac{\partial^2 \bar{\psi}}{\partial \bar{R}^2} + \frac{\partial \bar{\phi}}{\partial \bar{R}}\frac{\partial \bar{\psi}}{\partial \bar{R}} + \frac{\partial^2 \bar{\phi}}{\partial \bar{R}^2}\bar{\psi} \sim 2 + \left(C + 2\bar{R}\right)\frac{\partial \bar{\phi}}{\partial \bar{R}} + \left(C\bar{R} + \bar{R}^2\right)\frac{\partial^2 \bar{\phi}}{\partial \bar{R}^2},$$

which are the boundary conditions for $T$ and $\bar{\psi}$ as $\bar{R} \to \infty$.

5.3.2. *Boundary conditions as* $\bar{Z} \to \infty$

The region IV solutions must match to the region III solutions as $\bar{Z} \to \infty$. In region III, we obtained solutions in terms of a similarity variable $\eta$, and in terms of the region IV variables, $\bar{R}$ and $\bar{Z}$, the region III solutions are given by

$$T = T\left(\eta\right), \qquad \bar{\psi} = \left(3\bar{Z}\right)^{2/3} f\left(\eta\right), \qquad \text{where} \qquad \eta = \frac{\bar{R}}{\left(3\bar{Z}\right)^{1/3}}.$$

We require a boundary condition as $\bar{Z} \to \infty$, so we only need to know the structure of the solution in region III as $\eta \to 0$. We let

$$T = 1 + Q + \hat{T}, \qquad f = \hat{f},$$

where $\hat{T}$, $\hat{f}$ are small and substitute into (5.5), which gives

$$\frac{\mathrm{d}^2\hat{T}}{\mathrm{d}\eta^2} = 0, \quad \frac{\mathrm{d}^4\hat{f}}{\mathrm{d}\eta^4} = 0,$$

at leading order. The solutions are

$$\hat{T} = A_1\eta, \qquad \hat{f} = A_2\eta^3 + B_2\eta^2,$$

where we have satisfied the boundary conditions at $\eta = 0$, given in (5.6). The constants $A_1$, $A_2$ and $B_2$ are unknown but can be eliminated from the solutions to give mixed

boundary conditions of the form

$$\begin{aligned} \eta\frac{\mathrm{d}T}{\mathrm{d}\eta} - T &\to -(1+Q), \\ \frac{\eta^2}{6}\frac{\mathrm{d}^2 f}{\mathrm{d}\eta^2} - \frac{2\eta}{3}\frac{\mathrm{d}f}{\mathrm{d}\eta} + f &\to 0 \qquad\qquad \text{as} \qquad \eta \to 0. \\ -\eta^3\frac{\mathrm{d}^3 f}{\mathrm{d}\eta^3} + 4\eta^2\frac{\mathrm{d}^2 f}{\mathrm{d}\eta^2} - 10\eta\frac{\mathrm{d}f}{\mathrm{d}\eta} + 12f &\to 0, \end{aligned}$$

When these are written in terms of $\bar{\psi}$, $\bar{R}$ and $\bar{Z}$ we obtain

$$\begin{aligned} 3\bar{Z}\frac{\partial T}{\partial \bar{Z}} + T &\to 1+Q, \\ 3\bar{Z}\frac{\partial^2\bar{\psi}}{\partial\bar{Z}^2} + 4\frac{\partial\bar{\psi}}{\partial\bar{Z}} &\to 0, \qquad\qquad \text{as} \qquad \bar{Z}\to\infty. \\ 3\bar{Z}^2\frac{\partial^3\bar{\psi}}{\partial\bar{Z}^3} + 10\bar{Z}\frac{\partial^2\bar{\psi}}{\partial\bar{Z}^2} + 4\frac{\partial\bar{\psi}}{\partial\bar{Z}} &\to 0, \end{aligned}$$

These boundary conditions complete the system, which we solved using a numerical scheme similar to that outlined in Section 4.4.

### 5.4. *Numerical solution*

We checked the mesh dependency of the numerical solution, and found the maximum relative errors between solutions on different grids to be of $O(10^{-2})$. To minimise these errors without sufficiently increasing computational time we set $0 \leqslant \bar{R} \leqslant 12$, $\mathrm{d}\bar{R} = 0.1$, $-20 \leqslant \bar{Z} \leqslant 60$ and $\mathrm{d}\bar{Z} = 0.1$. We obtained results on this grid for a range of values of the wave speed, $C$, heat of reaction, $Q$, and mass flow rate, $\bar{q}$. We began by holding $Q$ and $\bar{q}$ constant and calculated the variation of critical temperature, $T_c$, with wave speed, $C$.

#### 5.4.1. *Variation of wave speed with critical temperature*

We obtained results for a range of values of $C$. The results for $C = 1$ and $C = 2$ are shown in Figures 16 and 17 respectively. The temperature profiles are qualitatively similar to those obtained in the constant density model. At the point where the reaction starts, $\bar{Z} = 0$, there is a displacement of the streamlines due to the changing density and viscosity of the gas mixture. This causes a large increase in the radial velocity around $\bar{R} = 0$, $\bar{Z} = 0$ as the heated gas moves away from the wall. This behaviour agrees with what we found in region II. The axial velocity also changes rapidly around $\bar{R} = 0$, $\bar{Z} = 0$ and increases as $\bar{Z}$ increases. From the solutions obtained at each value of the wave speed, $C$, we noted the critical temperature, $T_c$. The variation of $C$ with $T_c$ is plotted in Figure 18. The result is qualitatively similar to that obtained in the constant density model (see Figure 11). A quantitative comparison of the two models is made by looking at the variation of $T_c$ with heat released from the reaction, $Q$.

#### 5.4.2. *Variation of critical temperature with Q*

Our results for $Q$ sufficiently small must be consistent with the results we obtained using the constant density approximation, $Q \ll 1$, when the temperature was given by $T = 1 + Q\hat{T}$. For $C = 1$, $\bar{q} = 1$ we found that the critical temperature is $\hat{T}_c = 0.21$, and it follows that for small $Q$ the results of the compressible model for $T_c$ should be given approximately by $T_c = 1 + 0.21Q$. Figure 19 shows that solutions of the compressible model are in very good agreement with the constant density result when $Q$ is small, but

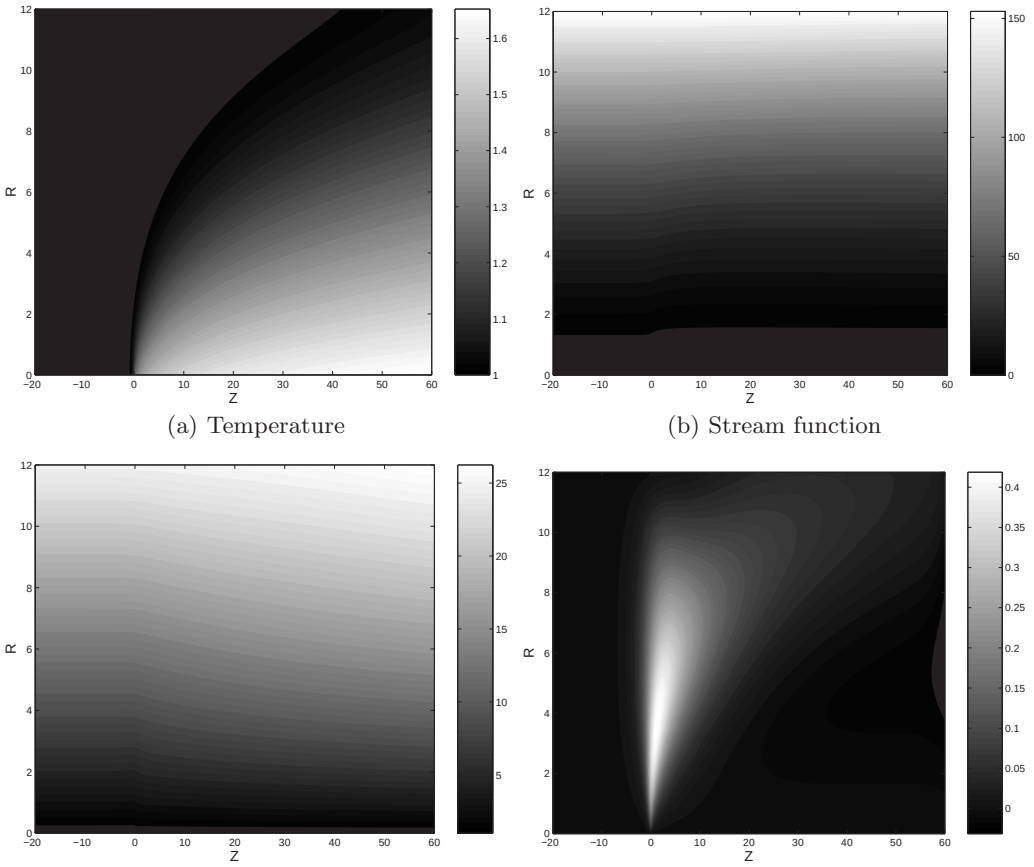


(a) Temperature (b) Stream function

(c) Axial velocity (d) Radial velocity

FIGURE 16. Region IV solutions for $C = 1$.

that for larger values of $Q$ the constant density approximation predicts too high a value for the critical temperature.

5.4.3. *Variation of wave speed with mass flow rate*

We now fix $Q$ and $T_c$ and vary the mass flow rate, $\bar{q}$, to see its effect on the wave speed, $C$. The results for $Q = 1$, $T_c = 1.2$ are shown in Figure 20. They are qualitatively similar to the constant density results shown in Figure 12. The wave speed decreases as $\bar{q}$ increases and reaches zero when $\bar{q} \approx 1.51$. For $\bar{q} > 1.51$ the wave speed is negative, so for sufficiently large mass flow rates, the reaction front propagates towards the outlet of the tube and will eventually be blown out.

## 6. Qualitative comparison with preliminary experiment

At present, only very limited experimental data is available. However, we can qualitatively compare the preliminary results obtained by Lefevre (2003) with our model. The experiment described in Section 1 was carried out several times using tubes of zirconia coated on their inner surface with varying amounts of platinum catalyst. The variation of the wave speed, $c^*$, with the amount of catalyst on the surface of the tube was measured and the results are given in Table 3. Two results linking the percentage of platinum on the

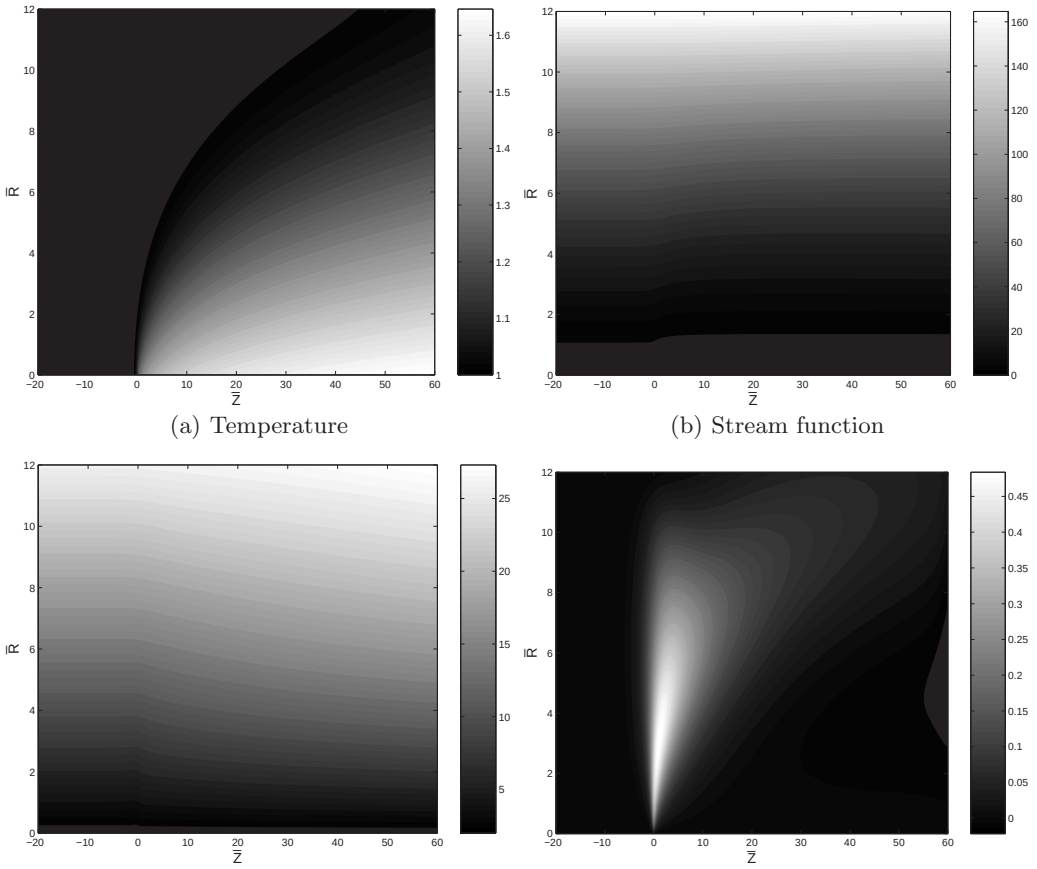


(a) Temperature (b) Stream function

(c) Axial velocity (d) Radial velocity

FIGURE 17. Region IV solutions for $C = 2$.

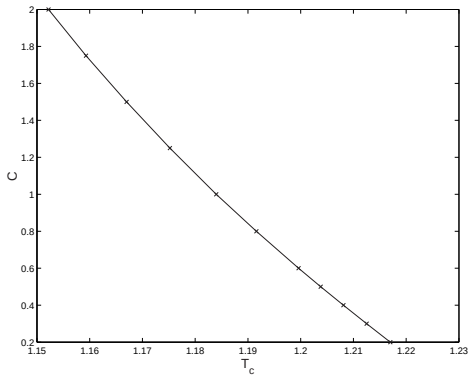


FIGURE 18. Plot of the wave speed, $C$, against critical temperature of reaction, $T_c$.

| | | | | |
|---|---|---|---|---|
| Percentage of platinum on surface of tube | 0.12 | 0.19 | 0.29 | 0.32 |
| Average wave speed (m $s^{-1} \times 10^{-4}$) | 0.80 | 1.65 | 1.95 | 2.65 |

TABLE 3. Experimental data.

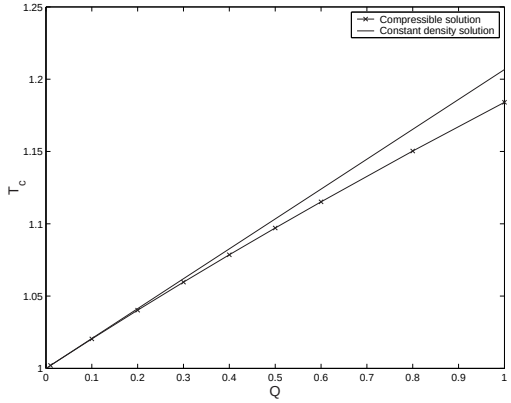


FIGURE 19. Plot of the critical temperature, $T_c$, against heat released from the reaction, $Q$.

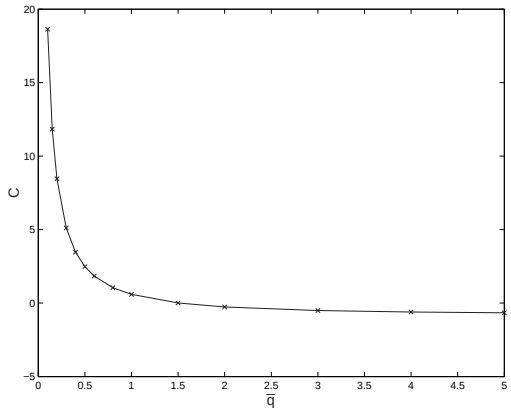


FIGURE 20. Plot of wave speed, $C$, against mass flow rate of fuel, $\bar{q}$.

tube to the critical temperature were obtained experimentally, and from these a linear relationship between the percentage platinum concentration, $P$, and critical temperature, $T^*$, was obtained, namely

$$T^* = -500P + 948.$$

Experimentally, the heat released from the reaction is large and gives $Q = O(10)$. However, our models are not valid for large values of $Q$, due to the simplification made in Section 2.4. By comparing the $Q = O(1)$ and constant density results, we know that as $Q$ increases to $O(1)$ values the constant density model predicts too high a critical temperature at constant wave speed, see Figure 19. From this we infer that as $Q$ increases to $O(10)$ values the $O(1)$ model will tend to overestimate the critical temperature. Therefore, as the wave speed decreases with increasing critical temperature, Figure 18, we conclude that the values of wave speed at each $T_c$ predicted by the $Q = O(1)$ model will be too high.

Indeed, the experimentally measured values of the wave speed are smaller than those predicted by our model, however, the qualitative behaviour of the results is the same; the wave speed decreases with increasing critical temperature.

Further experimental data relates the mass flow rate of fuel into the zirconia tube to the wave speed, as shown in Table 4. The experiments in this case were carried out using a tube coated with 0.4% platinum catalyst. Experimentally, as the mass flow rate increases

| | | | | | |
|---|---|---|---|---|---|
| Mass flow rate (kg $s^{-1} \times 10^{-6}$) | 1.09 | 1.63 | 2.18 | 2.72 | 3.27 |
| Average wave speed (m $s^{-1} \times 10^{-4}$) | 1.90 | 2.45 | 2.65 | 2.45 | 2.20 |

TABLE 4. Experimental data.

the wave speed increases until $q_{\text{in}}$ reaches a value of about $2 \times 10^{-6}$ kg $s^{-1}$. After this point, the wave speed decreases as the mass flow rate increases. Our asymptotic solution is based on a large mass flow rate, so we only expect to obtain agreement with experiment at sufficiently large values of $q_{\text{in}}$. Although, the wave speeds obtained from our model are again too large, the qualitative behaviour of the solutions for $q_{\text{in}} > 2 \times 10^{-6}$ is correct.

Furthermore, the numerical results show that for $q_{\text{in}}$ sufficiently large the wave speed becomes negative. Although the available experimental data does not show this, it has been reported that on increasing the mass flow rate sufficiently, the wave stops propagating towards the inlet and the reaction front is blown out of the tube.

We note that the work by Lefevre (2003) is at a very early stage and that the results need to be verified. Further work is also required to extend the experimental results to include a wider range of wave speeds, temperatures and mass flow rates, especially at large values of $q_{\text{in}}$.

## 7. Conclusion

We have shown that the reaction front, or surface-catalysed flame, that can propagate in a zirconia tube can be modelled as a steady travelling wave. We found that the speed of this reaction front decreases as the temperature at which the reaction starts, the critical temperature, $T_c$, increases, and as the mass flow rate of fuel entering the tube, $q_{\text{in}}$, increases. Having found a solution using the constant density approximation, we found that for larger values of the heat released by the reaction, $Q = O(1)$, the constant density model predicts too high a value for the wave speed, $C$. Also, as expected, the wave speeds predicted by our model were higher than those given by the experimental data. There is, however, qualitative agreement with experiment. At a critical value of the mass flow rate, $\bar{q} = \bar{q}_c$, the wave speed is zero and, as $\bar{q}$ increases past this critical value, $C$ becomes negative. Hence, for $\bar{q} > \bar{q}_c$ the reaction front propagates towards the outlet of the tube and the reaction will eventually be blown out. The experimental data available at present shows an increase in wave speed with mass flow rate, $q_{\text{in}}$, for small $q_{\text{in}}$ and then a decrease as $q_{\text{in}}$ increases past a value of about $2 \times 10^{-6}$ kg $s^{-1}$. Data at large values of the mass flow rate has not been obtained, although it has been observed experimentally that for large enough values of the mass flow rate the wave propagates towards the outlet of the tube and the reaction is blown out.

There are several possible extensions and improvements to the work in this paper. We hope to obtain better agreement between theory and experimental results by solving for larger values of $Q$, which could be done by considering the asymptotic solution for $Q \gg 1$. We could also consider some of the effects that we have currently neglected, such as heat loss from the tube, more realistic chemistry and electrochemistry. In addition to any further mathematical analysis, a validation of the current experimental results and more detailed experimental work is required. In particular, further results showing the variation of wave speed with large mass flow rate are needed to verify that the wave propagates backwards for sufficiently large $q_{\text{in}}$.

REFERENCES

Adamson, F. 2004 *Propagating reaction fronts in zirconia tubes* PhD Thesis, University of Birmingham.

Buckmaster, J. D. & Ludford, G. S. S. 1982 *Theory of Laminar Flames.* Cambridge University Press.

Carslaw, H. S. & Jaeger, J. C. 1959 *Conduction of Heat in Solids.* Oxford University Press.

Cooper, R. J. 2000 *Flow and reaction in solid oxide fuel cells* PhD Thesis, University of Birmingham.

Cooper, R. J., Billingham, J. & King, A. C. 2000 Flow and reaction in solid oxide fuel cells. *Journal of Fluid Mechanics* **411**, 233-262.

Davy, H. 1817 Some new experiments and observations on the combustion of gaseous mixtures, with an account of a method of preserving a continued light in mixtures of inflammable gases and air without a flame. *Phil. Trans. Roy. Soc. London* **107**, 77-85.

Finnerty, C. M., Cunningham, R. H., Kendall, K. & Ormerod, R. M. 1998 A novel test system for in situ catalytic and electrochemical measurements on fuel processing anodes in working solid oxide fuel cells. *Chemical Communications* **8**, 915-916.

Fletcher, C. A. J. 1991 *Computational Techniques for Fluid Dynamics, Volume I: Fundamental and General Techniques, Second Edition.* Springer-Verlag, Berlin.

John, F. 1978 *Partial Differential Equations, Third edition* Springer-Verlag, Berlin.

Kendall, K. & Prica, M. 1994 Integrated SOFC tubular system for small-scale cogeneration. *Proc.* $1^{st}$ *European Solid Oxide Fuel Cell Forum, Lucerne*, pp.163-170.

Kumar, R., Krumpelt, M. & Myles, K. M. 1992 Solid oxide fuel cells for transportation: a clean, efficient alternative for propulsion. *Proc.* $3^{rd}$ *International Symposium on Solid Oxide Fuel Cells* (ed. S. C. Singhal and H. Iwahara), pp.948-956, Pennington, NJ: The Electrochemical Society.

Lefevre, R. J. 2003 *Nanoparticle catalysts in fuel cells and fuel cell systems.* Internal report, School of Chemical Engineering, University of Birmingham.

Senkan, S. M. 1992 Detailed chemical kinetic modeling. *Advances in chemical engineering* (ed. J. Wei), **18**, 95-196, New York: Academic.

Singhal, S. C. & Kendall, K. 2003 *High Temperature Solid Oxide Fuel Cells: Fundamentals, Design and Applications.* Elsevier, Oxford.

Stewartson, K. 1964 *The Theory of Laminar Boundary Layers in Compressible Fluids.* Oxford University Press, London.

Winkler, W. 1994 SOFC-integrated power plants for natural gas. $1^{st}$ *European Solid Oxide Fuel Cell Forum* (ed. U. Bossel), **2**, 821-848, Lucerne: Kinzel.

## Appendix A. The additional asymptotic regions when $Q = O(1)$

### A.1. *Equations in region IIa*

We return to the original equations, (3.1), to determine the scalings for this new region. We remove the pressure terms from the momentum equations by differentiating (3.1b) with respect to $z'$ and (3.1c) with respect to $r$ and combining the resulting equations. We rescale the axial coordinate using $z' = \zeta\tilde{z}$ with $\zeta \ll 1$, and look for a WKB solution of the form

$$T = 1 + \epsilon^{\tilde{\gamma}} \exp\left(-\frac{\varphi(r,\tilde{z})}{\epsilon}\right),$$
$$\psi = -\left(r^2 - \frac{r^4}{2}\right) - Da^{-1}\frac{Cr^2}{2} + \tilde{\epsilon}^{\tilde{\delta}} \exp\left(-\frac{\tilde{\varphi}(r,\tilde{z})}{\tilde{\epsilon}}\right),$$

where $\epsilon$ and $\tilde{\epsilon}$ are small parameters and $\tilde{\gamma}$ and $\tilde{\delta}$ are constants. The streamfunction, $\psi$, is defined in exactly the same way as in region II. We substitute the expressions for $T$ and $\psi$ into the momentum and energy equations. This gives the leading order equations

for $\varphi$ and $\tilde{\varphi}$ as

$$-2(1-r^2)\frac{\partial\varphi}{\partial\tilde{z}} = \left(\frac{\partial\varphi}{\partial r}\right)^2 + \frac{1}{\bar{q}^2}\left(\frac{\partial\varphi}{\partial\tilde{z}}\right)^2, \tag{A 1a}$$

$$\begin{aligned} -2(1-r^2)\frac{\partial\tilde{\varphi}}{\partial\tilde{z}}&\left[\left(\frac{\partial\tilde{\varphi}}{\partial\tilde{z}}\right)^2 + \bar{q}^2\left(\frac{\partial\tilde{\varphi}}{\partial r}\right)^2\right]\exp\left(-\frac{\tilde{\varphi}}{\tilde{\epsilon}}\right) \\ &\qquad -4r\bar{q}^2(1-r^2)^2\frac{\partial\varphi}{\partial\tilde{z}}\frac{\partial\varphi}{\partial r}\exp\left(-\frac{\varphi}{\epsilon}\right) \\ = \left[2\left(\frac{\partial\tilde{\varphi}}{\partial r}\right)^2\left(\frac{\partial\tilde{\varphi}}{\partial\tilde{z}}\right)^2 + \frac{1}{\bar{q}^2}\left(\frac{\partial\tilde{\varphi}}{\partial\tilde{z}}\right)^4 + \bar{q}^2\left(\frac{\partial\tilde{\varphi}}{\partial r}\right)^4\right]&\exp\left(-\frac{\tilde{\varphi}}{\tilde{\epsilon}}\right) \\ +2r(1-r^2)\bar{q}^2\frac{\partial\varphi}{\partial r}&\left[\frac{1}{\bar{q}^2}\left(\frac{\partial\varphi}{\partial\tilde{z}}\right)^2 + \left(\frac{\partial\varphi}{\partial r}\right)^2\right]\exp\left(-\frac{\varphi}{\epsilon}\right), \end{aligned} \tag{A 1b}$$

where we have taken $\epsilon = \tilde{\epsilon} = \zeta = Da^{-2}$ and $\tilde{\delta} = \tilde{\gamma} + 1$. The viscosity and thermal conductivity are $\mu = T$ and $k = T$, as they were in region II. Using (A 1a), we cancel all the terms in $\varphi$ in (A 1b), which then reduces to

$$-2(1-r^2)\frac{\partial\tilde{\varphi}}{\partial\tilde{z}} = \left(\frac{\partial\tilde{\varphi}}{\partial r}\right)^2 + \frac{1}{\bar{q}^2}\left(\frac{\partial\tilde{\varphi}}{\partial\tilde{z}}\right)^2,$$

and is of the same form as (A 1a). The boundary conditions on $\varphi$ and $\tilde{\varphi}$ are identical,

$$\exp\left(-\frac{\varphi}{\epsilon}\right) \to 0, \qquad \text{as} \qquad \tilde{z} \to -\infty \qquad \text{and} \qquad r \to 0,$$

so we have $\tilde{\varphi} = \varphi$.

The solution in region IIa does not explicitly affect the solution in region IV, since region IIa has no boundaries with region IV (see Figure 14). The wave speed is determined in region IV and the variation of $C$ is the main result we wish to obtain from our model. Because of this, and the complexity of the problem, we will not look for a solution of (A 1a). However, in the correct asymptotic limits, the solution of (A 1a) satisfies the appropriate boundary conditions. We will show that, as $r \to 1$ and $z' \to 0$, (A 1a) reduces to the equations in region IIIa, which we now derive.

### A.2. *Region IIIa*

We again return to the original equations, (3.1), to determine the scalings for this new region. We eliminate the pressure from the momentum equations as we did in region IIa. We rescale using $r^2 = 1 - \xi R^*$, $z' = \tilde{\xi} Z^*$, with $\xi$, $\tilde{\xi} \ll 1$, and look for a WKB solution of the form

$$\begin{aligned} T &= 1 + \varepsilon^\gamma \exp\left(-\frac{\phi(R^*, Z^*)}{\varepsilon}\right), \\ \psi &= -\left(r^2 - \frac{r^4}{2}\right) - Da^{-1}\frac{Cr^2}{2} + \eta^\delta \exp\left(-\frac{\tilde{\phi}(R^*, Z^*)}{\eta}\right), \end{aligned}$$

where $\varepsilon$ and $\eta$ are small parameters and $\gamma$ and $\delta$ are constants. The streamfunction, $\psi$, is defined in exactly the same way as in regions II and IIa. Substituting the expressions for $T$ and $\psi$ into the momentum and energy equations, the leading order equations for

$\phi$ and $\tilde{\phi}$ are

$$-2R^*\frac{\partial\phi}{\partial Z^*} = 4\left(\frac{\partial\phi}{\partial R^*}\right)^2 + \frac{1}{\bar{q}^2}\left(\frac{\partial\phi}{\partial Z^*}\right)^2, \tag{A 2a}$$

$$\begin{aligned}-2R^*\frac{\partial\tilde{\phi}}{\partial Z^*}\left[\left(\frac{\partial\tilde{\phi}}{\partial Z^*}\right)^2 + 4\bar{q}^2\left(\frac{\partial\tilde{\phi}}{\partial R^*}\right)^2\right]\exp\left(-\frac{\tilde{\phi}}{\eta}\right) + 8R^{*2}\bar{q}^2\frac{\partial\phi}{\partial Z^*}\frac{\partial\phi}{\partial R^*}\exp\left(-\frac{\phi}{\varepsilon}\right)\\ = \left[8\left(\frac{\partial\tilde{\phi}}{\partial R^*}\right)^2\left(\frac{\partial\tilde{\phi}}{\partial Z^*}\right)^2 + \frac{1}{\bar{q}^2}\left(\frac{\partial\tilde{\phi}}{\partial Z^*}\right)^4 + 16\bar{q}^2\left(\frac{\partial\tilde{\phi}}{\partial R^*}\right)^4\right]\exp\left(-\frac{\tilde{\phi}}{\eta}\right)\\ -4R^*\bar{q}^2\frac{\partial\phi}{\partial R^*}\left[\frac{1}{\bar{q}^2}\left(\frac{\partial\phi}{\partial Z^*}\right)^2 + 4\left(\frac{\partial\phi}{\partial R^*}\right)^2\right]\exp\left(-\frac{\phi}{\varepsilon}\right),\end{aligned} \tag{A 2b}$$

where we have taken $\varepsilon = \eta = \tilde{\xi}\xi^{-3}$, $\bar{q} = q\,\tilde{\xi}\xi^{-1}$ and $\delta = \gamma + 2$. We fixed the magnitudes of these parameters by matching next order terms in the energy equation. The richest balance is obtained when $\varepsilon = Da^{-1}$, $\xi = Da^{-1/2}$ and $\tilde{\xi} = Da^{-5/2}$. All the terms in (A 2b) containing $\phi$ cancel due to (A 2a), and (A 2b) reduces to

$$-2R^*\frac{\partial\tilde{\phi}}{\partial Z^*} = 4\left(\frac{\partial\tilde{\phi}}{\partial R^*}\right)^2 + \frac{1}{\bar{q}^2}\left(\frac{\partial\tilde{\phi}}{\partial Z^*}\right)^2,$$

which is of the same form as (A 2a). The boundary conditions on $\phi$ and $\tilde{\phi}$ are identical,

$$\exp\left(-\frac{\phi}{\varepsilon}\right) \to 0 \qquad \text{as} \qquad Z^* \to -\infty, \qquad \text{and} \qquad R^* \to \infty, \tag{A 3}$$

so we conclude that $\tilde{\phi} = \phi$.

A.2.1. *Matching regions IIa and IIIa*

The equation for $\varphi$ in region IIa, (A 1a), should reduce to (A 2a) as $r \to 1$, $\tilde{z} \to 0$. Substituting for $R^*$ and $Z^*$ into (A 1a), we obtain

$$-2R^*\frac{\partial\phi}{\partial Z^*} = 4\left(\frac{\partial\phi}{\partial R^*}\right)^2 + \frac{1}{\bar{q}^2}\left(\frac{\partial\phi}{\partial Z^*}\right)^2,$$

to leading order, where $\phi = Da^{1/2}\varphi$, and this is identical to (A 2a). The region IIa solution for the temperature is given by

$$T = 1 + Da^{-\tilde{\gamma}}\exp\left(-Da\,\varphi\right),$$

and in region IIIa we have

$$T = 1 + Da^{-\gamma/2}\exp\left(-Da^{1/2}\phi\right),$$

and, since $\phi = Da^{1/2}\varphi$, the exponential term is the same in both regions. The term in front of the exponential will be affected by the next order solutions for $\phi$ and $\varphi$ so at leading order it is not necessary for these two terms to match. We conclude that the leading order temperatures in regions IIa and IIIa match as $R^*$, $|Z^*| \to \infty$. In a similar manner it follows that the streamfunctions also match to leading order.

### A.3. *Solution for $\phi$*

We solve (A 2a) by writing it as a system of characteristic ordinary differential equations in terms of a parameter $t$ (John 1978). Rewriting (A 2a) as

$$F\left(R^*, Z^*, \phi, \mathcal{P}, \mathcal{Q}\right) = 2R^*\mathcal{Q} + 4\mathcal{P}^2 + \frac{1}{\bar{q}^2}\mathcal{Q}^2 = 0, \tag{A 4}$$

where

$$\mathcal{P} = \frac{\partial \phi}{\partial R^*}, \qquad \mathcal{Q} = \frac{\partial \phi}{\partial Z^*},$$

the characteristic equations are then given by

$$\frac{\mathrm{d}R^*}{\mathrm{d}\,t} = 8\mathcal{P}, \quad \frac{\mathrm{d}Z^*}{\mathrm{d}\,t} = 2R^* + \frac{2\mathcal{Q}}{\bar{q}^2}, \quad \frac{\mathrm{d}\phi}{\mathrm{d}\,t} = -2R^*\mathcal{Q}, \quad \frac{\mathrm{d}\mathcal{P}}{\mathrm{d}\,t} = -2\mathcal{Q}, \quad \frac{\mathrm{d}\mathcal{Q}}{\mathrm{d}\,t} = 0.$$

On solving these, we obtain

$$R^* = -8at^2 + 8bt + f, \tag{A 5a}$$

$$Z^* = -\frac{16}{3}at^3 + 8bt^2 + 2ft + \frac{2at}{\bar{q}^2} + g, \tag{A 5b}$$

$$\phi = \frac{16}{3}a^2t^3 - 8abt^2 - 2aft + h, \tag{A 5c}$$

$$\mathcal{P} = -2at + b, \tag{A 5d}$$

$$\mathcal{Q} = a, \tag{A 5e}$$

where $a$, $b$, $f$, $g$ and $h$ are functions of $s$ that satisfy

$$\frac{\mathrm{d}h}{\mathrm{d}s} = b(s)\frac{\mathrm{d}f}{\mathrm{d}s} + a(s)\frac{\mathrm{d}g}{\mathrm{d}s},$$

and (A 4) when $t = 0$. A simple solution is

$$a = s, \qquad b = s, \qquad f = -2s - \frac{1}{2\bar{q}^2}s, \qquad g = 2s + \frac{1}{2\bar{q}^2}s, \qquad h = 0,$$

and (A 5)(a)-(c) become

$$R^* = -8st^2 + 8st - 2s - \frac{1}{2\bar{q}^2}s, \tag{A 6a}$$

$$Z^* = -\frac{16}{3}st^3 + 8st^2 - 4st + \frac{1}{\bar{q}^2}st + 2s + \frac{1}{2\bar{q}^2}s, \tag{A 6b}$$

$$\phi = \frac{16}{3}s^2t^3 - 8s^2t^2 + 4s^2t + \frac{1}{\bar{q}^2}s^2t. \tag{A 6c}$$

Dividing (A 6b) by (A 6a) eliminates $s$ and, after rearranging the result, we obtain a cubic equation for $t$,

$$t^3 - \frac{3}{2}\left(\frac{Z^*}{R^*} + 1\right)t^2 + \frac{3}{2}\left(\frac{Z^*}{R^*} + \frac{1}{2} - \frac{1}{4\bar{q}^2}\right)t - \frac{3}{8}\left(\frac{Z^*}{R^*} + \frac{1}{4\bar{q}^2}\frac{Z^*}{R^*} + 1 + \frac{1}{4\bar{q}^2}\right) = 0. \tag{A 7}$$

On solving this, the solution for $t$ can be substituted into (A 6c) and, using (A 6a) to eliminate $s$, we obtain

$$\phi = \frac{4\bar{q}^2R^{*2}\left(16\bar{q}^2t^3 - 24\bar{q}^2t^2 + 12\bar{q}^2t + 3t\right)}{3\left(16\bar{q}^2t^2 - 16\bar{q}^2t + 4\bar{q}^2 + 1\right)^2}. \tag{A 8}$$

The appropriate root of (A 7) is determined by the boundary conditions on $\phi$ as $Z^* \to -\infty$ and $R^* \to \infty$, given in (A 3). Figure 21 shows the real and imaginary parts of

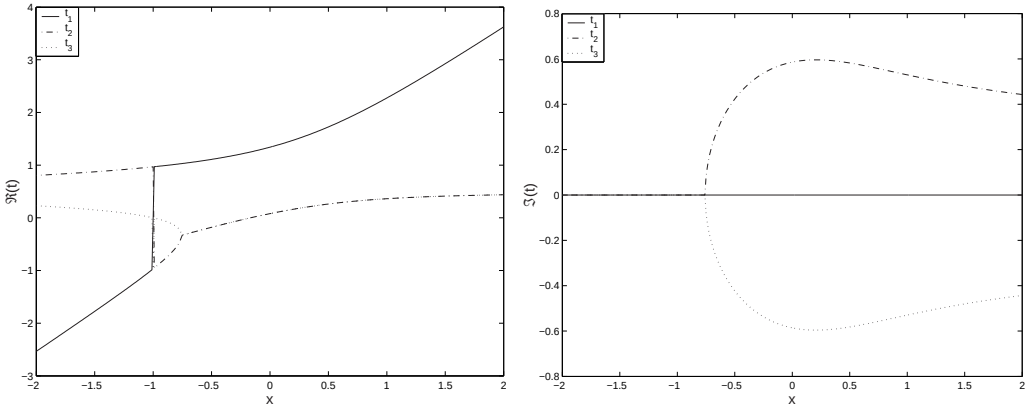


(a) $\Re(t)$ (b) $\Im(t)$

FIGURE 21. Roots of the cubic equation, (A 7).

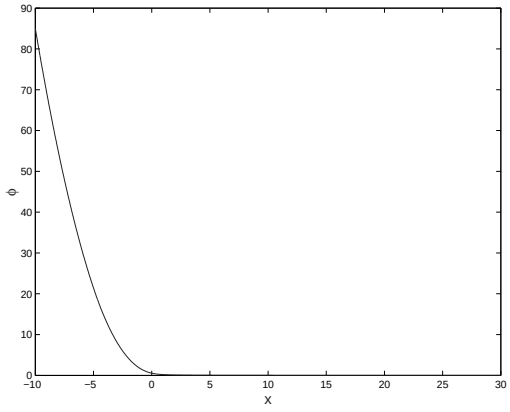


FIGURE 22. Solution for $\phi$.

the roots of (A 7) for a range of values of $x = Z^*/R^*$. We take the real, positive root, which for $x > -1$ is $t_1$, shown as the solid line in the figure, and for $x \leqslant -1$ is $t_2$, the dashed curve in the figure. The solution for $\phi$, after making this choice for $t$, is shown in Figure 22.

The solution in region IIIa is therefore given by

$$T = 1 + Da^{-\gamma} \exp\left(-Da\,\phi\right),$$
$$\psi = -\frac{1}{2} - Da^{-1}\frac{C}{2} + Da^{-3/2}\frac{CR^*}{2} + Da^{-1}\frac{R^{*2}}{2} + Da^{-(\gamma+2)} \exp\left(-Da\,\phi\right),$$

where $\phi$ is given by (A 8) and $t$ is the root of (A 7) which gives the correct behaviour of $\phi$ at each point $(R^*, Z^*)$ as described. We must compare this solution to the numerical solution in region II to determine whether they match in the appropriate limit.

A.3.1. *Matching between regions II and IIIa*

As we match to region II, the region IIIa variables become large and positive. The correct solution of (A 7) in this case is given by

$$t = \frac{1}{4R^*\bar{q}}\mathcal{T} + \frac{1}{4R^*\bar{q}}\left(R^{*2} + 4\bar{q}^2 Z^{*2}\right)\frac{1}{\mathcal{T}} + \frac{1}{2}\frac{Z^* + R^*}{R^*},$$

where $\mathcal{T}$ is given by

$$\mathcal{T} = \Big(2\bar{q}\left(4\bar{q}^2+3\right)R^{*3} + 6\bar{q}Z^*R^{*2} + 8\bar{q}^3\bar{Z}^{*3} + R^*\Big[\left(64\bar{q}^6+96\bar{q}^4+36\bar{q}^2-1\right)R^{*4} + \left(96\bar{q}^4+72\bar{q}^2\right)R^{*3}Z^* + 24\bar{q}^2R^{*2}Z^{*2} + \left(128\bar{q}^6+96\bar{q}^4\right)R^*Z^{*3} + 48\bar{q}^4Z^{*4}\Big]^{1/2}\Big)^{1/3}.$$

In terms of the region II variables we find that to leading order

$$t \sim \frac{3}{2}Da^2\frac{z'}{(1-r^2)}.$$

Substituting this into the expression for $\phi$ and taking the leading order terms we get

$$\phi \sim Da^{-1}\frac{(1-r^2)^3}{18z'}.$$

The region IIIa solutions in terms of $r$ and $z'$ are therefore

$$T = 1 + Da^{-\gamma}\exp\left(-\frac{(1-r^2)^3}{18z'}\right), \tag{A 9a}$$

$$\psi = -\left(r^2-\frac{r^4}{2}\right) + Da^{-\gamma-2}\exp\left(-\frac{(1-r^2)^3}{18z'}\right), \tag{A 9b}$$

to leading order. We expect that the small correction to the solution in region IIIa will give an $O(1)$ contribution in region II to match with the numerical solution obtained here. The multiplier in front of the exponential term could be found from the next order solution for $\phi$, and the value of $\gamma$ chosen to make this term $O(1)$ in region II. However, our solution for $T$ satisfies

$$\frac{\partial T}{\partial z'} = \frac{(1-r^2)^3}{18z'^2}(T-1),$$

which gives the leading order behaviour for $T$, at small $z'$, without calculating the next order correction for $\phi$. Similarly, the small $z'$ behaviour of the streamfunction, $\psi$, is given by

$$\frac{\partial \psi}{\partial z'} = \frac{(1-r^2)^3}{18z'^2}\left(\psi + \left(r^2-\frac{r^4}{2}\right)\right).$$

Substituting the region II solution into the expressions

$$f_T = z'^2\frac{\partial T}{\partial z'} - \frac{(1-r^2)^3}{18}(T-1),$$

$$f_\psi = z'^2\frac{\partial \psi}{\partial z'} - \frac{(1-r^2)^3}{18}\left(\psi + \left(r^2-\frac{r^4}{2}\right)\right),$$

we expect to find that $f_T$ and $f_\psi \to 0$ as $z' \to 0$. Figure 23 shows these functions for small $z'$, confirming that the solutions in regions II and IIIa match in the limit $z' \to 0$.

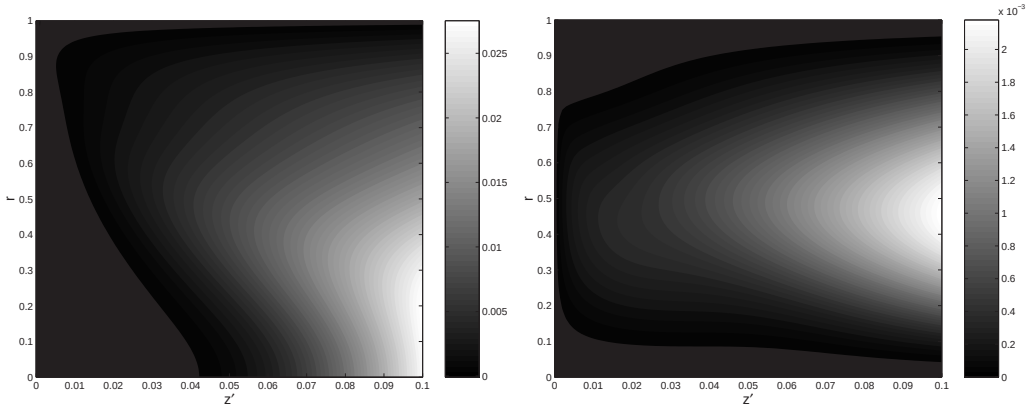


(a) $f_T$ (b) $f_\psi$

FIGURE 23. Comparison between solutions in regions II and IIIa.